U.S. DEPARTMENT OF COMMERCE
National Technical Information Service

PB-288 234

Poilutant Emissions from 'Dirty' Low- and Medium-Btu Gases

Institute of Gas Technology, Chicago, IL

Prepared for

Industrial Environmental Research Lab, Research Triangle Park, NC

Oct 78

United States
Environmental Protection
Agency

Industrial Environmental Research
Laboratory
Research Triangle Park NC 27711

EPA-600/7-78-191
October 1978

PB 288234

EPA

Pollutant Emissions from "Dirty" Low- and Medium-Btu Gases

Interagency Energy/Environment R&D Program Report

REPRODUCED BY
NATIONAL TECHNICAL
INFORMATION SERVICE
U. S. DEPARTMENT OF COMMERCE
SPRINGFIELD, VA. 22161

86

RESEARCH REPORTING SERIES

Research reports of the Office of Research and Development, U.S. Environmental Protection Agency, have been grouped into nine series. These nine broad categories were established to facilitate further development and application of environmental technology. Elimination of traditional grouping was consciously planned to foster technology transfer and a maximum interface in related fields. The nine series are:

1. Environmental Health Effects Research
2. Environmental Protection Technology
3. Ecological Research
4. Environmental Monitoring
5. Socioeconomic Environmental Studies
6. Scientific and Technical Assessment Reports (STAR)
7. Interagency Energy-Environment Research and Development
8. "Special" Reports
9. Miscellaneous Reports

This report has been assigned to the INTERAGENCY ENERGY-ENVIRONMENT RESEARCH AND DEVELOPMENT series. Reports in this series result from the effort funded under the 17-agency Federal Energy/Environment Research and Development Program. These studies relate to EPA's mission to protect the public health and welfare from adverse effects of pollutants associated with energy systems. The goal of the Program is to assure the rapid development of domestic energy supplies in an environmentally-compatible manner by providing the necessary environmental data and control technology. Investigations include analyses of the transport of energy-related pollutants and their health and ecological effects; assessments of, and development of, control technologies for energy systems; and integrated assessments of a wide range of energy-related environmental issues.

REVIEW NOTICE

This report has been reviewed by the participating Federal Agencies, and approved for publication. Approval does not signify that the contents necessarily reflect the views and policies of the Government, nor does mention of trade names or commercial products constitute endorsement or recommendation for use.

This document is available to the public through the National Technical Information Service, Springfield, Virginia 22161.

TECHNICAL REPORT DATA
(Please read Instructions on the reverse before completing)

1. REPORT NO. EPA-600/7-78-191	2.
3. RECIPIENT'S ACCESSION NO. PB288234	
4. TITLE AND SUBTITLE Pollutant Emissions from "Dirty" Low- and Medium-Btu Gases	5. REPORT DATE October 1978
	6. PERFORMING ORGANIZATION CODE
7. AUTHOR(S) R.T. Waibel, E.S. Fleming, and D.H. Larson	8. PERFORMING ORGANIZATION REPORT NO.
9. PERFORMING ORGANIZATION NAME AND ADDRESS Institute of Gas Technology Applied Combustion Research IIT Center, 3424 South State Street Chicago, Illinois 60616	10. PROGRAM ELEMENT NO. EHE624A 11. CONTRACT/GRANT NO. 68-02-2643
12. SPONSORING AGENCY NAME AND ADDRESS EPA, Office of Research and Development Industrial Environmental Research Laboratory Research Triangle Park, NC 27711	13. TYPE OF REPORT AND PERIOD COVERED Final; 5/77-4/78 14. SPONSORING AGENCY CODE EPA/600/13

15. SUPPLEMENTARY NOTES IERL-RTP project officer is David G. Lachapelle, Mail Drop 65, 919/541-2236. EPA-600/7-77-094a and -094b are earlier reports in this series.

16. ABSTRACT The report gives results of a study to determine the emissions from 'dirty' low- and medium-Btu gases when combusted on industrial process burners. The fuels tested were blends with compositions typical of Wellman-Galusha oxygen (WGO) and air (WGA) fuel gases. Baseline data were collected for natural gas, ambient WGO and WGA, and hot WGO (700 K) and WGA (616 K). Ammonia, H_2S, coal tar, and char were added to the hot fuels to determine their effects on pollutant emissions. Study conclusions include: (1) low-Btu fuels not subjected to post-gasifier cleanup can yield NOx levels greatly above the thermal levels for the clean fuels and for natural gas; (2) in turbulent diffusion flames, fuel-NOx increases with an increase in a) the amount of fuel-nitrogen, b) the amount of fuel-sulfur, c) the level of excess air, and d) the degree of initial fuel/air mixing; (3) attempts to close the fuel-sulfur balance were unsuccessful (further work should be done in this area); and (4) compared to natural gas, heat transfer to the load is reduced for the low-Btu fuels tested (this heat transfer is not greatly affected by the presence of contaminants--tar and char--at levels characteristic of raw gasifier effluents).

17. KEY WORDS AND DOCUMENT ANALYSIS

a. DESCRIPTORS	b. IDENTIFIERS/OPEN ENDED TERMS	c. COSATI Field/Group
Air Pollution	Air Pollution Control	13B
Nitrogen Oxides	Stationary Sources	07B
Fuels	Low-Btu Gas	21D
Burners	Medium-Btu Gas	13A
Industrial Processes	Dopants	13H
Combustion		21B
Additives		11G

18. DISTRIBUTION STATEMENT Unlimited	19. SECURITY CLASS *(This Report)* Unclassified	21. NO. OF PAGES 86
	20. SECURITY CLASS *(This page)* Unclassified	22. PRICE PCA05/MF A01

EPA Form 2220-1 (9-73)

EPA-600/7-78-191

October 1978

Pollutant Emissions from "Dirty" Low- and Medium-Btu Gases

by

R. T. Waibel, E. S. Fleming, and D. H. Larson

Institute of Gas Technology
Applied Combustion Research
IIT Center, 3424 South State Street
Chicago, Illinois 60616

Contract No. 68-02-2643
Program Element No. EHE624A

EPA Project Officer: David G. Lachapelle

Industrial Environmental Research Laboratory
Office of Energy, Minerals, and Industry
Research Triangle Park, NC 27711

Prepared for

U.S. ENVIRONMENTAL PROTECTION AGENCY
Office of Research and Development
Washington, DC 20460

CONTENTS

	Page
Abstract	iv
Executive Summary	v
Figures	vi
Tables	viii
1. Introduction	1
2. Test Facilities	10
3. Experimental Plan	20
4. Results	25
Natural gas: base-line tests	25
Wellman-Galusha oxygen: emission studies	35
Wellman-Galusha air: emission studies	49
Particulate studies	53
Furnace efficiency	58
5. Discussion	68
Fuel-nitrogen effects on NO_x	68
Fuel-sulfur effects on NO_x	71
References	74
Conversion Table	76

ABSTRACT

When low-Btu fuels, resulting from coal gasification, are not subjected to post-gasifier cleanup, their combustion can result in NO_x levels greatly above the clean fuel values. In general, for turbulent diffusion combustion the level of NO_x increases with an increase in a) the amount of fuel-nitrogen, b) the amount of fuel-sulfur, c) the level of excess air, and d) the degree of initial fuel/air mixing. Besides enhancing NO_x, fuel-sulfur is converted to SO_x. Results can be interpreted to support the contention that, in the presence of NO_x, large amounts of SO_3 may be formed in turbulent diffusion flames characterized by poor fuel/air mixing. Further research is needed, however, to definitely determine the fate of fuel sulfur in this type of flame.

EXECUTIVE SUMMARY

Data were collected to determine the emissions from "dirty" low- and medium-Btu gases when combusted on industrial process burners. The fuels utilized were blended to have the composition typically found for Wellman-Galusha oxygen (WGO) and air (WGA) fuel gases. Base-line data were collected for natural gas, ambient WGO and WGA, and hot WGO (700K) and WGA (616K). Then ammonia, hydrogen sulfide, coal tar and char were added singly at various levels and in combinations to the hot fuels in a parametric study to determine the effects of these contaminants on pollutant emissions. The burners used in this study were a forward-flow baffle burner and a gas momentum controlled kiln burner. These burners were mounted in turn on a pilot-scale test furnace equipped with water tubes as a load and were each fired at 1.03 ± 0.07 MW_t ($3.50 \pm 0.25 \times 10^6$ Btu/hr) with 10% excess air and 477 K (400°F) air preheat.

Based on a detailed analysis of the experimental data the following conclusions were made:

- Low-Btu fuels not subjected to post-gasifier cleanup can yield NO_x levels greatly above the thermal levels for the clean fuels and for natural gas.
- In turbulent diffusion flames, fuel-NO_x increases with an increase in a) the amount of fuel-nitrogen, b) the amount of fuel-sulfur, c) the level of excess air, and d) the degree of initial fuel/air mixing.
- Attempts to close the fuel-sulfur balance were unsuccessful. Whether this shortfall is due to sampling/instrument effects or large concentrations of some unmeasured sulfur-containing species is not clear. Further work should be done in this area.
- Compared to natural gas, heat transfer to the load is reduced for the low-Btu fuels tested. This heat transfer is not greatly affected by the presence of contaminants (tar and char) at levels characteristic of raw gasifier effluents.

FIGURES

Number		Page
1	Comparison of fuel conversion processes	3
2	Sulfur removal from coal during gasification	6
3	Nitrogen removal from coal during gasification	8
4	Pilot-scale test furnace	11
5	Overall furnace system	13
6	Doping system to synthesize "dirty" low-btu gases	15
7	Assembly drawing of the suction pyrometer	16
8	Assembly drawing of gas sampling probe	18
9	RAC "Staksamplr" schematic of EPA particulate sampling train (Method 5)	19
10	Bloom baffle burner	28
11	Assembly drawing of baffle burner	29
12	Profile of five-zone reheating furnace with overhead metal recuperator	29
13	Scaled drawing of test furnace with cooling-tube positions for PBB simulation	31
14	Heat-absorption profile of preheat section of a five-zone reheat furnace as a function of furnace length	32
15	Schematic drawing of a rotary cement kiln	33
16	Temperature and composition in a typical cement kiln	33
17	Heat absorption profile of reaction and calcining zones of a rotary cement kiln	34
18	Scaled drawing of test furnace with cooling tube positions for FMCB simulation	36
19	Schematic diagram of the kiln burner fuel injector	37
20	Ammonia conversion for Wellman-Galusha oxygen fuel gas on the baffle burner with 10% and 20% excess air	44

FIGURES, Cont.

Number		Page
21	Ammonia conversion for Wellman-Galusha oxygen fuel gas on the kiln burner with 10% and 20% excess air	45
22	Effect of H_2S on ammonia (1.0% by volume) conversion to NO_x with Wellman-Galusha oxygen (10% excess air)	47
23	Effects of radial vs. axial flow on ammonia (1.0%) conversion to NO_x with Wellman-Galusha oxygen fuel gas on the kiln burner	48
24	Particulate emissions for char doping of Wellman-Galusha fuel gases on the baffle and kiln burners (10% excess air)	55
25	Heat absorption profiles for ambient, "clean" Wellman-Galusha oxygen and natural gas on the baffle burner	59
26	Heat absorption profiles for hot "clean" Wellman-Galusha oxygen and natural gas on the baffle burner	60
27	Heat absorption profiles for ambient, clean Wellman-Galusha air and natural gas on the baffle burner	61
28	Heat absorption profiles for hot, clean Wellman-Galusha air and natural gas on the baffle burner	62
29	Heat absorption profile for ambient, clean Wellman-Galusha oxygen and natural gas on the kiln burner	63
30	Heat absorption profile for hot, clean Wellman-Galusha oxygen and natural gas on the kiln burner	64
31	Heat absorption profile for Wellman-Galusha air fuel gas compared to natural gas on the kiln burner	66
32	Heat absorption profile for hot, clean Wellman-Galusha air and natural gas on the kiln burner	67

TABLES

Number		Page
1	Primary Converters — Distribution of Energy into Products and By-Products	4
2	Tar Analysis	9
3	Char Analysis	9
4	Fuel Composition for Low- and Medium-Btu Gases Tested	14
5	Summary of Test Data for Baffle Burner	26
6	Summary of Test Data for Kiln Burner	27
7	Base-Line Data for Clean Fuels: Natural Gas and Wellman-Galusha Oxygen (WGO), 3.5 Million Btu/hr With 10% Excess Air	38
8	Char Doping: Wellman-Galusha Oxygen (700 K), 3.5 Million Btu/hr With 10% Excess Air	40
9	Tar Doping: Wellman-Galusha Oxygen (700 K), 3.5 Million Btu/hr With 10% Excess Air	41
10	Ammonia Conversion to NO_x on the Baffle Burner	42
11	Ammonia Conversion to NO_x on the Kiln Burner	43
12	Parametric Doping: Wellman-Galusha Oxygen (700 K), 3.5 Million Btu/hr With 10% Excess Air	50
13	Parametric and "Dirty" Doping: Wellman-Galusha Oxygen (700 K), 3.5 Million Btu/hr With 10% Excess Air	51
14	Base-Line Data for Clean Fuels: Natural Gas and Wellman-Galusha Air (WGA), 3.5 Million Btu/hr With 10% Excess Air	52
15	"Dirty" Doping: Wellman-Galusha Air (616 K), 3.5 Million Btu/hr With 10% Excess Air	54
16	Baffle Burner Cascade Impactor Results for Char-Doped Wellman-Galusha Oxygen (700 K) — Doping Rate: 1.14 g/s	56
17	Kiln Burner Cascade Impactor Results for Char-Doped Wellman-Galusha Oxygen (700 K) — Doping Rate: 0.76 g/s	57

INTRODUCTION

The objective of the research program was to provide and evaluate quantitative data on the differences in the environmental quality of effluent combustion products and furnace efficiency when retrofitting a natural gas/oil industrial burner with "dirty" intermediate- and low-Btu gases. These data were collected from the IGT pilot-scale industrial test furnace.

This program was intended to complement a recently completed EPA program,[15] which evaluated the emissions resulting from burning "clean" low- and medium-Btu gases in boilers. This previous work provided quantitative information on emissions using gases processed by ambient temperature sulfur cleanup systems and enabled correlating emissions to gas composition and operating conditions.

Work is currently being done by the government and industry to develop high temperature-post gasification sulfur cleanup systems. This is an attractive development because it would enable utilizing the sensible heat contained in the product gas from the gasifier. The high-temperature cleanup processes leave varying amounts of tars, oils, and ammonia in the product gas stream. Since these contaminants can contribute to emissions resulting from combustion of fuel gas, it is important that the magnitude of the potential problem be evaluated and the results used to determine if high-temperature sulfur removal systems are feasible from an environmental viewpoint. A cursory look at the combustion process emissions using a "dirty" intermediate-Btu gas reveals a potential increase in the NO_x emission level from 50 ppm to 500 ppm. Thus, before a decision on the suitability of retrofitting gas/oil-fired industrial burners with "dirty" intermediate- and low-Btu gases can be made, experimental values on NO_x emissions must be available and evaluated relative to emission standards.

A second area of concern when retrofitting an industrial furnace with intermediate- or low-Btu gases is loss in furnace efficiency. This decrease in efficiency could arise due to a decrease in flame emissivity, lower adiabatic flame temperature, and increased volume of combustion products. "Dirty" low- and intermediate-Btu gases could have higher flame emissivities than "clean" gases due to tar-oils and char, which could result in increased

furnace efficiency. However, the ambient "clean" fuel often has a higher adiabatic flame temperature due to a lower water content in the fuel. This program was designed to quantify such changes in efficiency and provide data on which a decision can be made on retrofitting an industrial process furnace with low- or intermediate-Btu gases.

This program was designed to provide data for two (2) gases and two (2) burners as a means to broadly scope the potential environmental problem.

ENVIRONMENTAL ASSESSMENT OF COMMERCIAL GASIFICATION PROCESSES

Tars and Oils

A wide variety of coal conversion systems can be used to produce a low- or intermediate-Btu gas. However, the operating conditions of the gasifier and cleanup system will have a significant effect upon the types of potential pollutants present in the off-gas. In most of the gasification processes, the initial treatment of the coal determines the major characteristics of the raw gas. These initial treatment conditions are illustrated by the temperature-pressure coordinates of Figure 1. Initial dimensions of contact time, gas-to-coal ratio, contacter types (entrained bed, fluidized-bed, fixed-bed, stirred liquid), and contacter mode (cocurrent, countercurrent, back-mixed reactor), and perhaps other variables should be included for a complete profile, but Figure 1 can be used to gain insight as to the types of pollutants, particularly higher organic compounds that might be present in the raw gasifier product.

Comparison of Figure 1 with Table 1 indicates how the initial operating regimes of the various processes affect the products of the individual converters, particularly the quantities of tars and oils that are present in the raw off-gas. These tars and oils may contain a variety of high-molecular-weight materials.

These liquids would be condensed and removed from the gas stream using ambient temperature sulfur cleanup systems, but would not be removed when using the high-temperature processes. If not condensed they would be burned during the combustion process with the off-gas. The combustion of these tar- and oil-containing gases in an environmentally acceptable manner was part of the overall experimental evaluation.

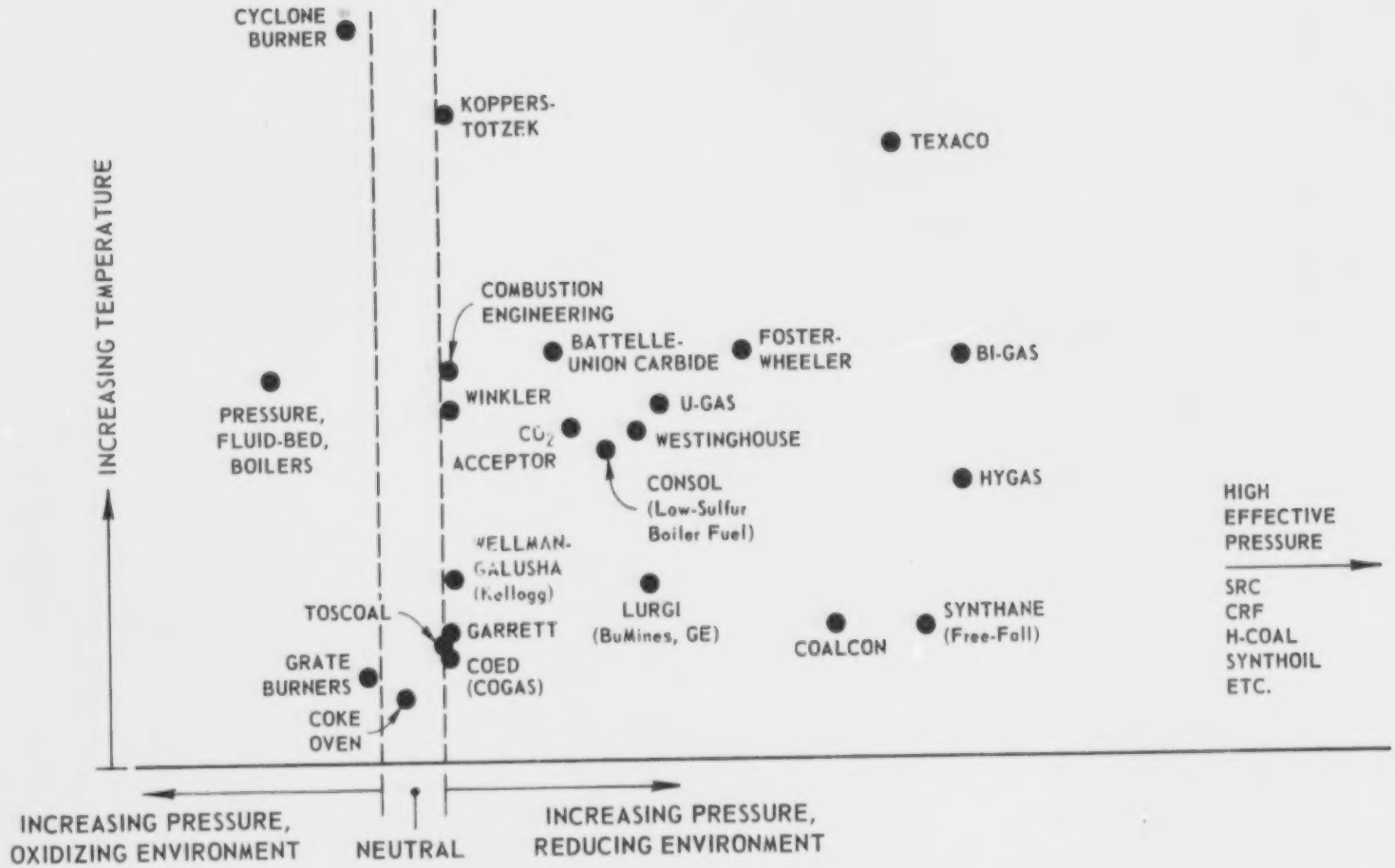

Figure 1. Comparison of fuel conversion processes

The basic character of the complex coal organic structure is aromatic. Therefore, the tars that are expelled from coal during devolatilization in lower temperature reactors may be expected to contain naphthalenes, indenes, anthracenes, and similar compounds. Oxygenated compounds such as phenols and cresylic acids may be expected, in addition to nitrogen- and sulfur-containing ring structures. In moderate temperature reactors, these complex aromatics are hydrocracked and possibly hydrodealkylated to simpler BTX (benzene-toluene-xylene) streams.

TABLE 1. PRIMARY CONVERTERS — DISTRIBUTION OF ENERGY INTO PRODUCTS AND BY-PRODUCTS

	Percent of Output Energy		
Process	Gas	Tars and Oils	Chars, Ash, and Residue
Koppers-Totzek	95	--	5
Texaco	95	--	5
U-Gas	96	--	4
BI-GAS	95	--	5
CO_2-Acceptor	94	--	6
HYGAS-Oxygen	95	3	2
Synthane	71	4	25
Westinghouse	96	--	4
Union Carbide	96	--	4
Winkler	80	--	20
Wellman-Galusha	72	18	10
Lurgi	69	16	15
COED	25	20	55
TOSCOAL	6	18	76
Garrett	35	15	60
H-COAL	10	75	15
CSF	10	75	5
SCR	20	55	25

Of the conversion processes illustrated in Figure 1 and listed in Table 1, only four are commercially available: Koppers-Totzek, Winkler, Wellman-Galusha, and Lurgi. Of these, only Wellman-Galusha and Lurgi produce significant amounts of tars and oils.

Sulfur

The sulfur that is present in coal is one of the primary reasons that low- and intermediate-Btu gasification processes are being developed. Much of the coal in this country contains significant quantities of sulfur, and present methods of sulfur oxides reduction, such as stack-gas scrubbing, are not viewed as sufficiently reliable, effective, or operable by many potential coal users. The concept of low- and intermediate-Btu gasification permits the removal of the sulfur from the gas before combustion, and overall sulfur oxides emissions may be significantly reduced utilizing this approach. The other major impetus for the development of low- and intermediate-Btu gasification is the higher overall efficiency achieved when the gas is utilized to produce electricity in combined-cycle operations.

The sulfur that occurs naturally in the coal will be largely driven into the raw product gas, as illustrated in Figure 2. These data are based upon analyses of the initial coal and gasification residues; hard data do not exist on the form of the sulfur in the off-gas.

Thermodynamically, the great majority of the sulfur should exist as hydrogen sulfide, with approximately 4% of the sulfur existing as carbonyl sulfide (COS) and only trace amounts of carbon disulfide. However, the thermodynamics are based upon gas-phase equilibria and may not be applicable in the gasification system. In most calculations of moderate-temperature gasifier operations, the gas-solids reactions are assumed to occur, but only a limited number of gas-gas reactions will occur at temperatures below the range of 1144 to 1366 K (1600° to 2000°F). Data available from Texaco and Koppers-Totzek coverters indicate that the COS-H_2S equilibrium is attained; comparable data from coke ovens, however, indicate that the concentrations of COS and CS_2 are much higher than would be expected thermodynamically. The disposition of the sulfur in the gas in moderate-temperature gasifiers cannot be accurately predicted at this time.

Purification systems are available for removing a large quantity of the hydrogen sulfide that is present in the raw product gas. Currently, much work is being done to develop and demonstrate the use of high-temperature sulfur clean-up systems. However, even the most optimistic projections show an H_2S concentration of 100 ppm in the off-gas.

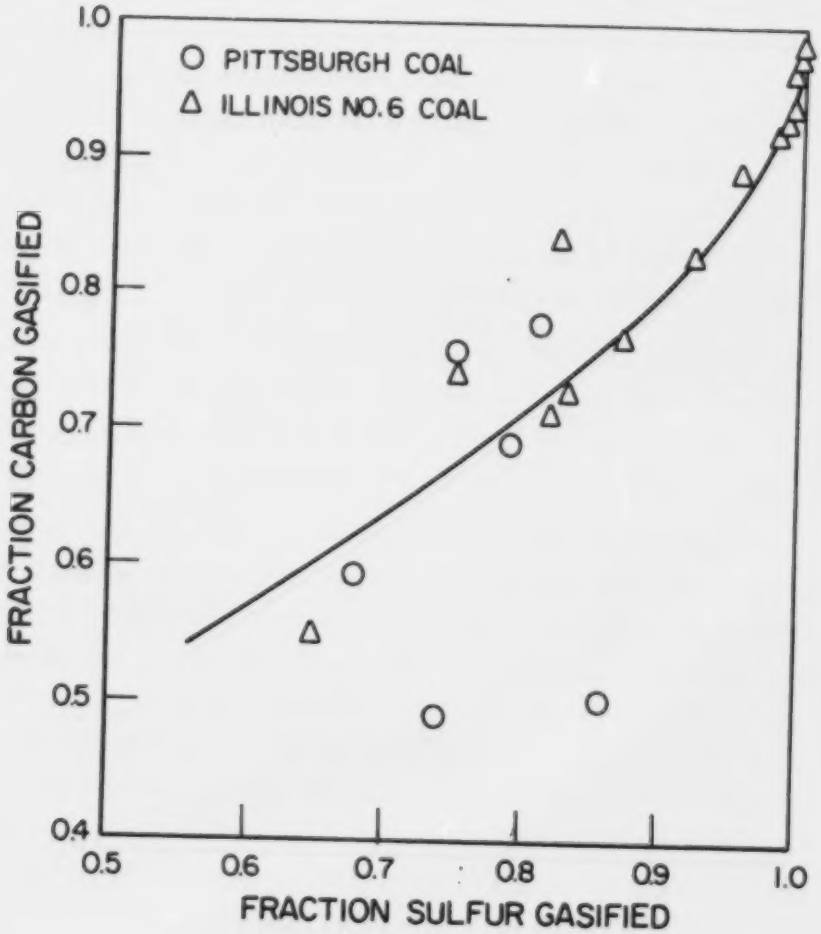

Figure 2. Sulfur removal from coal during gasification[5]

Nitrogen

Nitrogen that is present in coal may be considered as fixed nitrogen. Fixed nitrogen may be defined as nitrogen that is chemically bound to other species in contrast to molecular nitrogen (N_2) that is present in the air. The nitrogen in coal tends to gasify simultaneously with the carbon,[8] as illustrated in Figure 3. Generally, the nitrogen is expected to react with the hydrogen during gasification to form ammonia. The existence of ammonia in raw gasifier effluents has been confirmed by many investigators.

Hydrogen cyanide (HCN) is also present in the raw gas effluents. Published data report concentrations of less than 10% of the ammonia concentration. Thus, the major contribution in NO_x formation will be ammonia.

Although a number of potential pollutants might be present in the raw gasifier products, the data now available on their occurrence and/or concentration are poor. Consequently, the trials concentrated on the fate of species for which some data exists (tars, oils, ammonia, particulate, and hydrogen sulfide). These contaminants were "doped" into the hot experimental fuel gas. Although coal-tar does not have an identical chemical analysis to that of tars and oils found in raw off-gas, it does contain all the aromatic and oxygenated compounds that are found. Thus, realistic characterization of the combustion process and pollutant emissions can be anticipated. Analyses of the tar and char are presented in Tables 2 and 3.

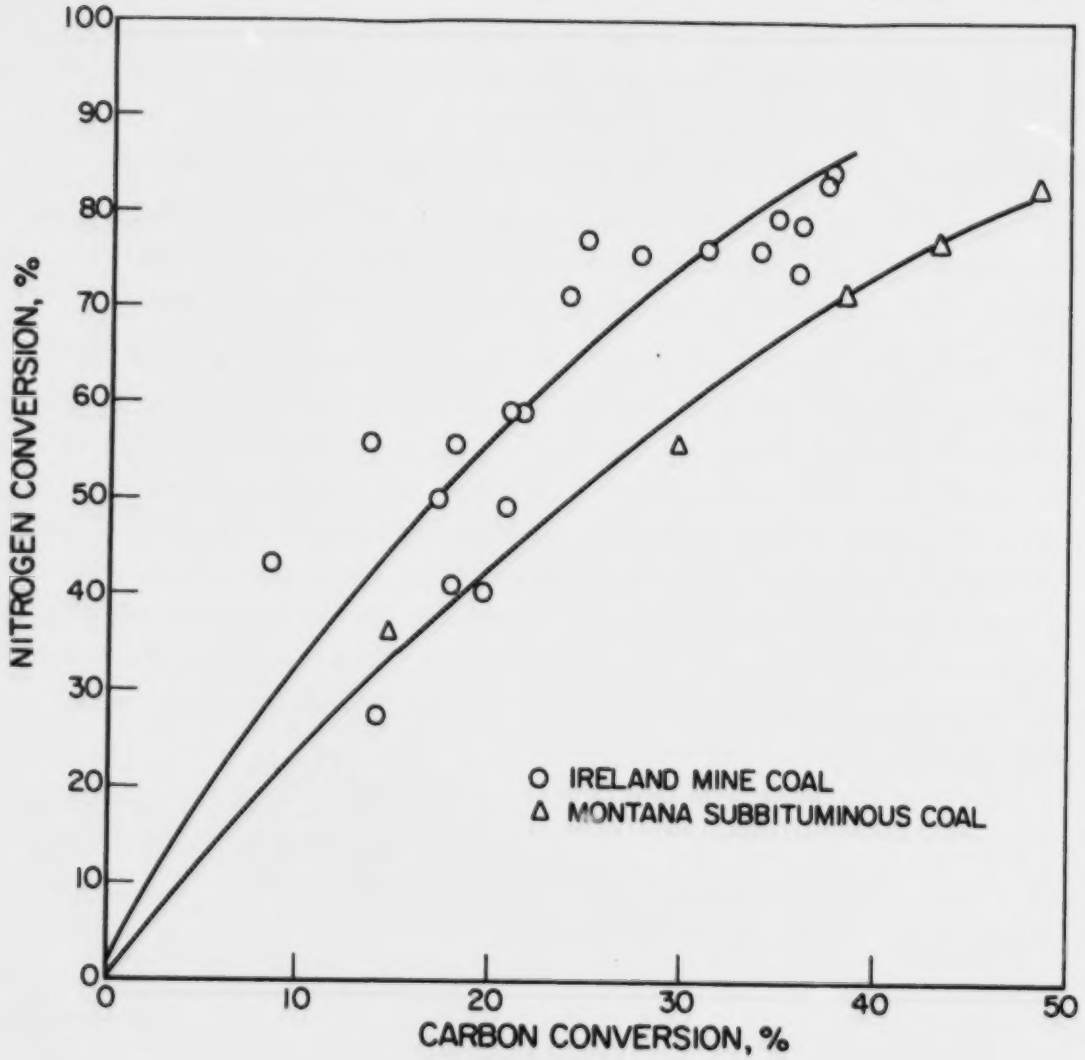

Figure 3. Nitrogen removal from coal during gasification[8]

TABLE 2. TAR ANALYSIS

Ultimate Analysis	Wt % (Dry Basis)
Ash	0.0
Carbon	84.39
Hydrogen	5.65
Sulfur	0.47
Nitrogen	0.55
Oxygen (by difference)	8.94

General Analysis	Wt % (As Received)
Solids	27.1
Heavy Fraction	55.3
Light Fraction (Toluene, Benzene, Xylene)	17.6

TABLE 3. CHAR ANALYSIS

Ultimate Analysis	Wt % (Dry Basis)
Ash	22.88
Carbon	66.30
Hydrogen	1.75
Sulfur	1.78
Nitrogen	0.72
Oxygen (by difference)	6.57

Proximate Analysis	Wt % (As Received)
Moisture	7.8
Volatile Matter	13.6
Ash	21.1
Fixed Carbon	57.5

Sieve Analysis	Wt % Retained
Screen	
200	67.7
230	3.3
270	4.9
325	3.6
Pan	20.5

TEST FACILITIES

PILOT-SCALE FURNACE

The experimental work was carried out in the pilot-scale furnace shown in Figure 4. This furnace is 14 feet* long and has a cross-sectional area of 21.3 sq ft. The facility can be used for firing burners rated up to 6 million Btu/hr (6M Btu/hr). Combustion air temperatures up to 1000°F can be generated with a separately fired air preheater.

The furnace is also equipped with 58 water cooling tubes, each of which can be independently inserted through the roof, along the sidewalls. Varying the number of tubes, their location, and the depth of insertion allows control over the magnitude and character of the load that can be placed on the furnace. The amount of heat absorbed by each tube can be determined by measuring the water flow through each tube and the temperature difference between the inlet and outlet. The water temperature measurements are made with a Vertronix digital thermometer. The stated accuracy is 0.25°F. These measurements were checked with a mercury-in-glass thermometer, accurate to 0.1°F, and were found to agree within 0.2°F. A temperature difference of 25° to 60°F was maintained between the water inlet and outlet. This helped minimize the effect of temperature measurement error on the heat balance. The water flow rate from each tube was determined by measuring the time to fill a bucket of known capacity. The time was measured using a quartz digital stopwatch.

In addition to the combustion air preheater, a separately fired fuel preheater is available that can heat 12,000 SCFH of low-Btu gas to any desired temperature up to 800°F. Temperatures up to 1200°F are attainable with lower flow rates.

---

* It is EPA policy to use metric units. However, in this report, English units are occasionally used for convenience. See conversion table at back of this volume.

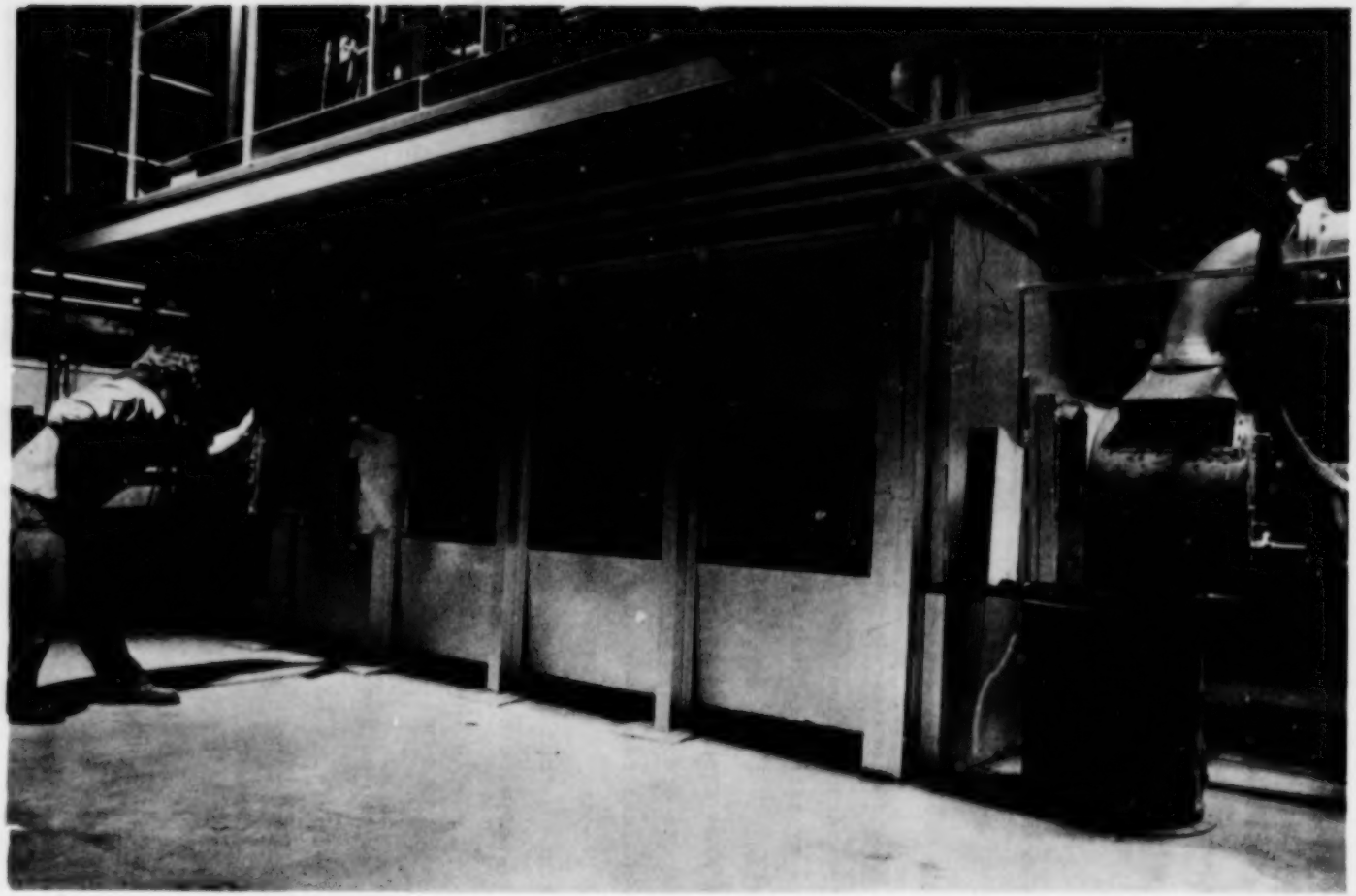

Figure 4. Pilot-scale test furnace

The overall system, shown in Figure 5, has the flexibility to independently vary —

- Fuel firing rate
- Air input
- Furnace load
- Air preheat temperature
- Fuel preheat temperature.

There are 33 panels or "sampling doors," shown in Figure 4, along one sidewall that allow insertion of probes at any axial position from the burner wall to the rear wall.

LOW-Btu GAS GENERATING SYSTEM

The low- and medium-Btu gases are generated using a special gas-generating and fuel-preparation facility. The critical items are the special gas generators or reformers that can produce varying ratios of hydrogen and carbon monoxide. Natural gas, carbon dioxide, and steam are passed through reaction retorts contained in a vertical cylindrical furnace. The catalyst-filled retorts are heated by the furnace and the input gases undergo endothermic chemical reactions at a temperature of 1422 K (2100°F). The gases are then quenched and compressed (maximum 80 psig). Facilities are available to remove excess carbon dioxide, if necessary. After compression, the product gas is blended with nitrogen, methane, carbon dioxide, and/or steam, as required, to obtain the specified composition of the fuel gas to be tested.

Up to 1.69×10^6 J/s (5.75 million Btu/hr) of simulated low- or medium-Btu fuel gas can be generated. This corresponds to 0.39 m^3/s (50,000 SCFH) of 4.29×10^6 J/m^3 (115 Btu/ft^3) low-Btu gas. Table 4 gives the composition of the Wellman-Galusha oxygen (WGO) and Wellman-Galusha air (WGA) fuel gases, which were chosen to be simulated as test gases for the program.

DOPANT SYSTEM

Figure 6 gives a schematic diagram of the doping system. Raw coal-tar from a coke oven was used as the tar introduced into the hot gas stream. Ammonia and hydrogen sulfide were blended into the fuel gas stream from cylinders. The flow of these dopants was adjusted using rotameters. The tar,

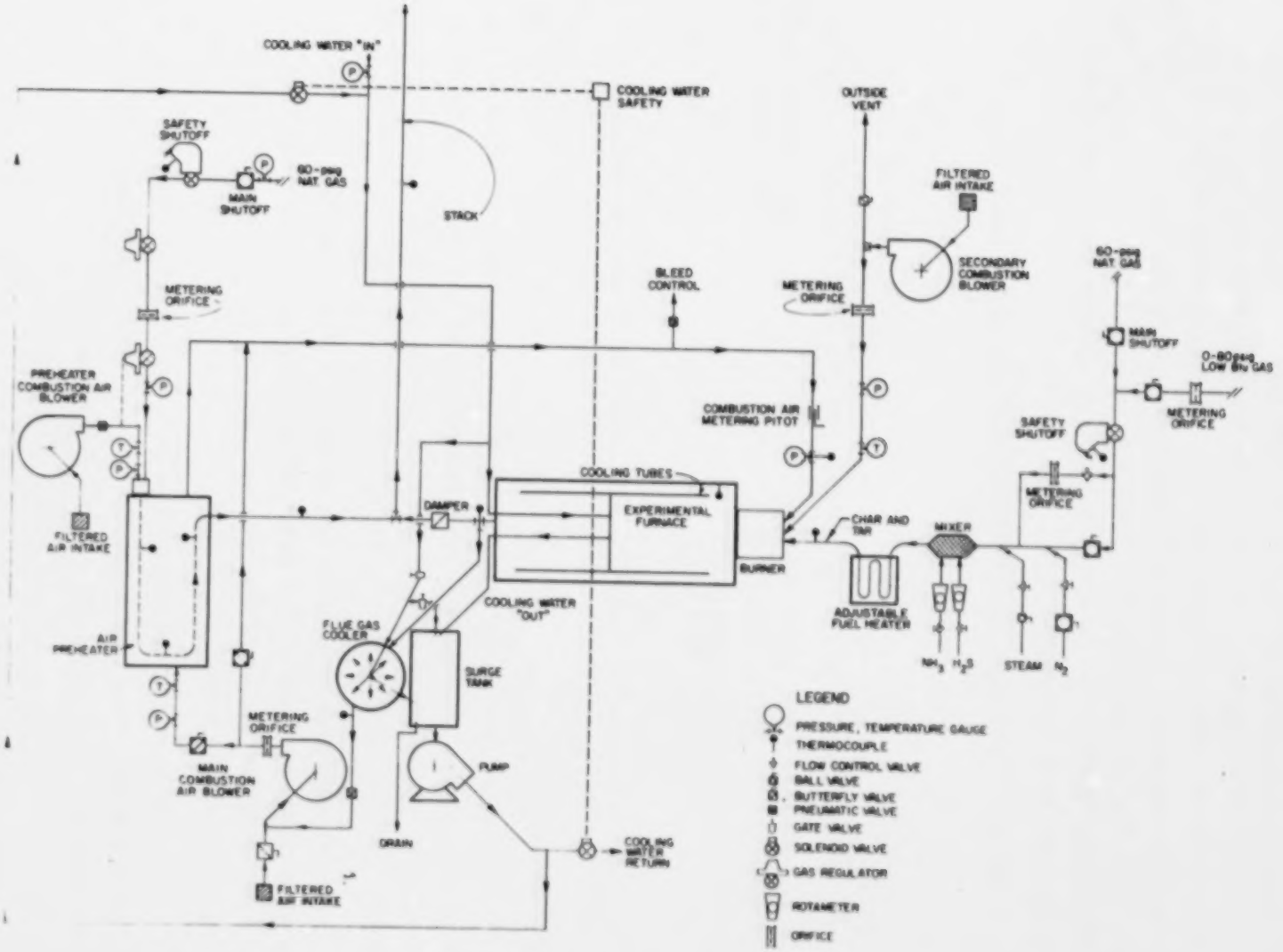

Figure 5. Overall furnace system

which was a liquid at room temperature, was forced from a container under nitrogen pressure through a nozzle in the hot fuel feed line where it was steam atomized. The tar nozzle was about 2 m from the nozzle exit. Feed rates were continually monitored by measuring the weight loss of tar from the pressurized feed tank over time. Char was screw-fed into the hot fuel, the feeder being about 2.5 m from the nozzle exit. Doping rates were controlled by varying the screw speed.

TABLE 4. FUEL COMPOSITION FOR LOW- AND MEDIUM-Btu GASES TESTED

Fuel	Temp, °F	CO	H_2	CO_2	CH_4	N_2	H_2O	Heating Value, Btu/SCF	Adiabatic Flame Temp,* K (°F)
Wellman-Galusha Oxygen	90	39.2	40.4	16.2	0.9	1.4	1.9	267	2248 (3587)
	800	29.7	30.6	12.4	0.7	1.1	25.5	202	2190 (3483)
Wellman-Galusha Air	90	26.9	14.3	7.4	2.6	46.9	1.9	159	2045 (3222)
	650	25.2	13.4	6.9	2.4	44.1	8.0	149	2044 (3220)

* 10% excess air at 477 K (400°F). The adiabatic flame temperature for ambient (298 K, 77°F) natural gas is 2231 K (3556°F).

INSTRUMENTATION

A major task of this program is to measure temperature profiles at the flue and flue-gas composition. Modified designs of the International Flame Reserach Foundation were used to construct probes that enabled this type of data collection.

Temperature data were collected using a suction pyrometer; the design is illustrated in Figure 7. A Pt/Pt-13% Rh thermocouple was used. The efficiency of the pyrometer was monitored and was better than 95% with a 15-second response time.

The flow direction was measured using a water-cooled Hubbard probe, with the upstream and downstream pressure taps connected to a Datametrics Barocel transducer and Datametrics CGS electric manometer.

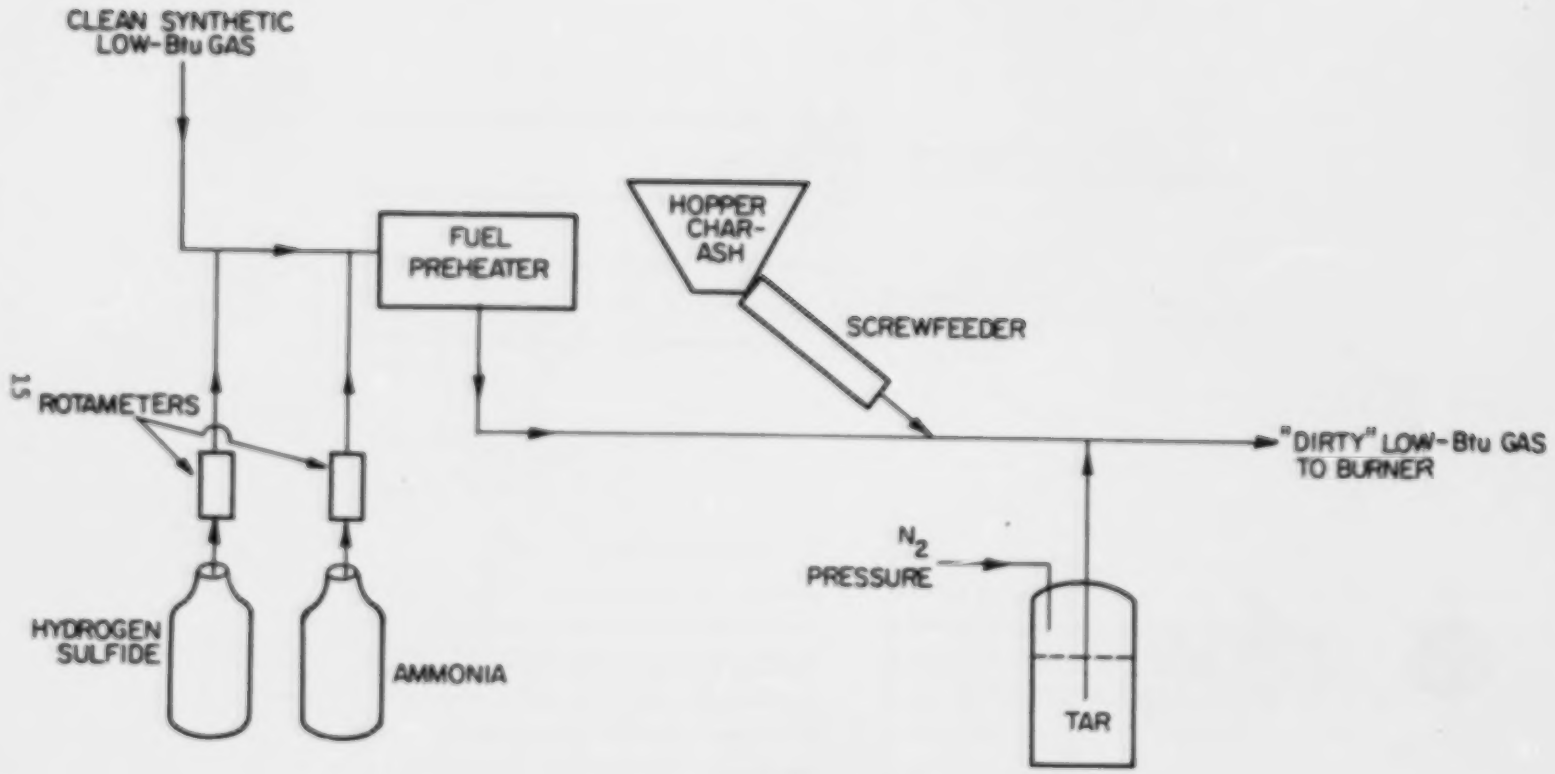

Figure 6. Doping system to synthesize "dirty" low-btu gases

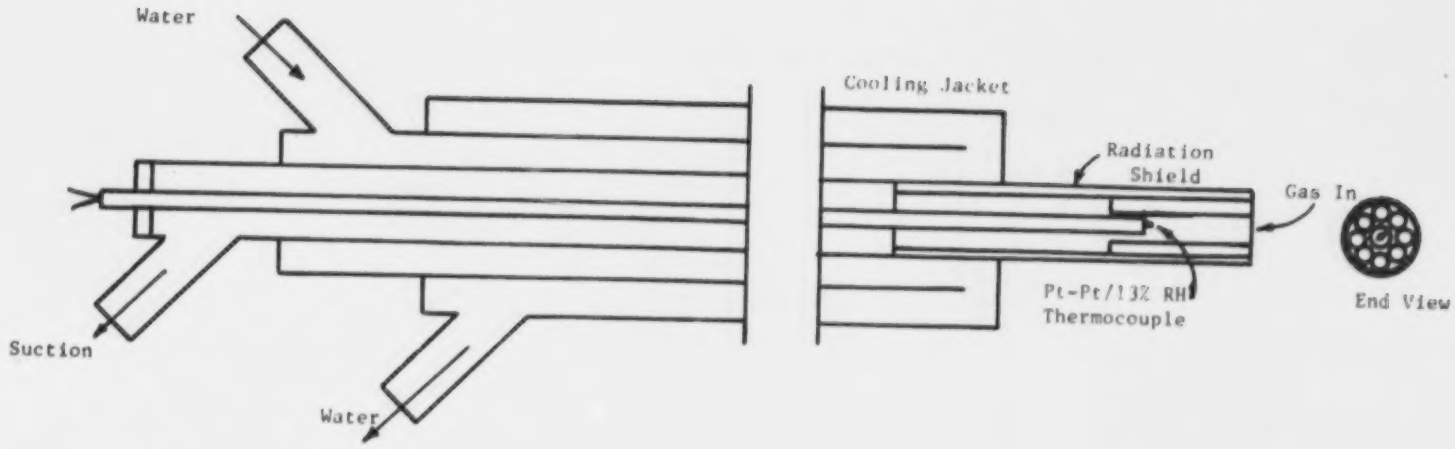

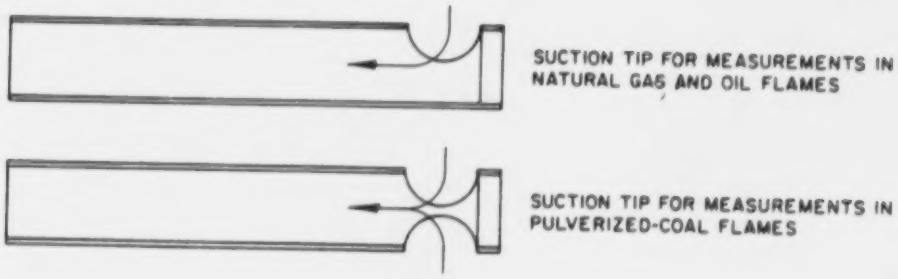

Alternate Probe Tips

Figure 7. Assembly drawing of the suction pyrometer

Figure 8 shows the assembly drawing of the gas-sampling probe used in the flame and the flue. To minimize NO_2 losses, the probe is water-cooled stainless steel joined to a Teflon® sample line. At the end of the probe is a section of Teflon tube heated to 190°F, followed by a Millipore filter and a Permapure® gas dryer. This dryer reduces the dew point to less than 32°F. In the dryer, water in the sample gas diffuses through a thin membrane into a stream of dry nitrogen. Tests have shown that only water is lost from the sample stream.

The analytic instrumentation equipment consists of the following items:

- Beckman 742 Polarographic Oxygen (O_2)
- Beckman Paramagnetic Oxygen (O_2)
- Beckman NDIR Methane (CH_4)
- Beckman NDIR Carbon Monoxide (CO)
- Beckman NDIR Carbon Dioxide (CO_2)
- Varian 1200 Flame Ionization Chromatograph (Total CH and C_2 to C_9)
- Beckman NDIR Nitric Oxide (NO)
- Beckman UV Nitrogen Dioxide (NO_2)
- Thermo Electron Pulsed Flourescent Sulfur Dioxide (SO_2)
- Hewlett-Packard Thermoconductivity Chromatography, Hydrogen (H), Nitrogen (N_2), Argone (A_2), CO, CO_2, C_1 to C_5, Oxygen (O_2)
- Beckman Chemiluminescent NO-NO_2
- Data Integration System.

To evaluate radiation intensity, which is needed for determination of flame emissivity, a PR 200 Pyroelectric radiometer, manufactured by Molectron Corp. in Sunnyvale, California, was used. This radiometer uses a permanently poled lithium tantalate detector that is capable of resolving radiant power in the nanowatt range while maintaining a continuous spectral response from the vacuum UV to 500 μm. A built-in optical calibration system, in the form of a highly stable LED (light-emitting diode) that is calibrated against an NBS traceable standard of total irradiance, permits a direct correlation of experimental data from different trials.

To measure stack particulates, a Research Appliance Corp. (RAC) Model 2414 "Staksamplr" sampling train (Figure 9) was employed. To provide greater

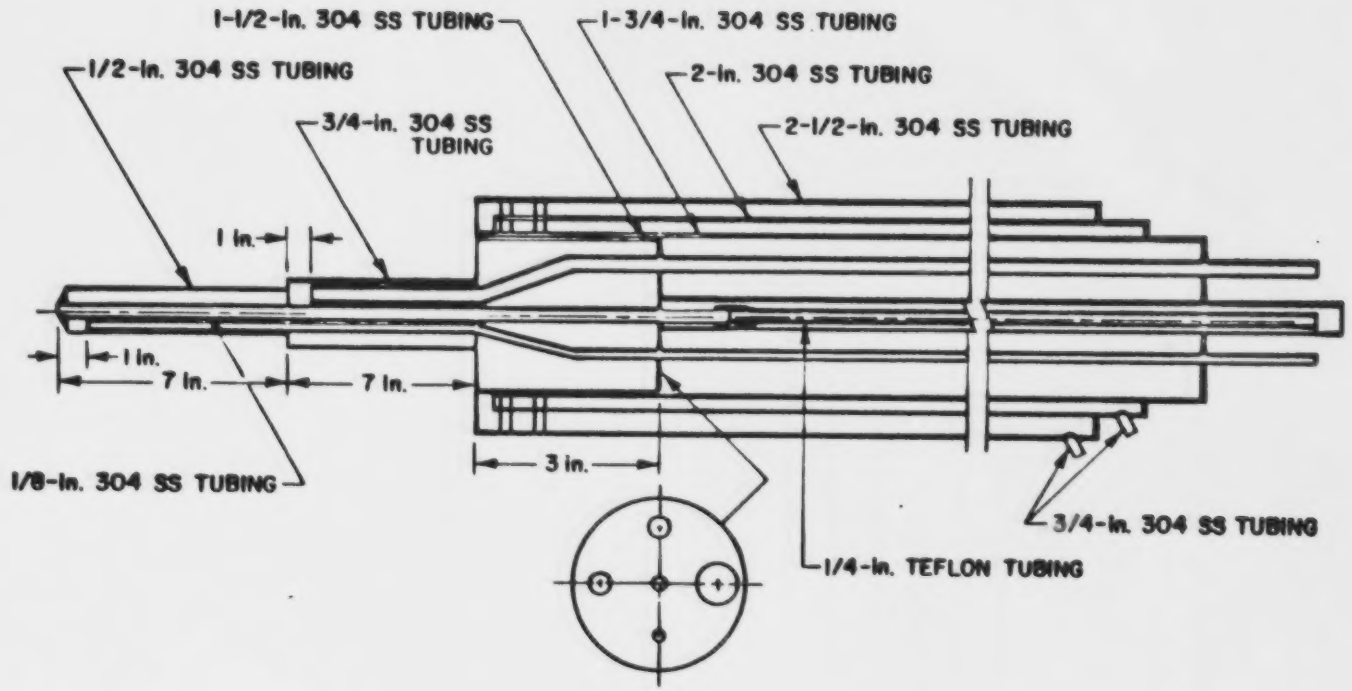

Figure 8. Assembly drawing of gas sampling probe

accuracy in measuring stack-gas velocity, the differential pressure of the stack-gas velocity probe was measured by a Barocel differential pressure transducer rather than the inclined manometer originally provided with the RAC instrument. The output of the pressure transducer was electronically amplified and recorded continuously during a trial.

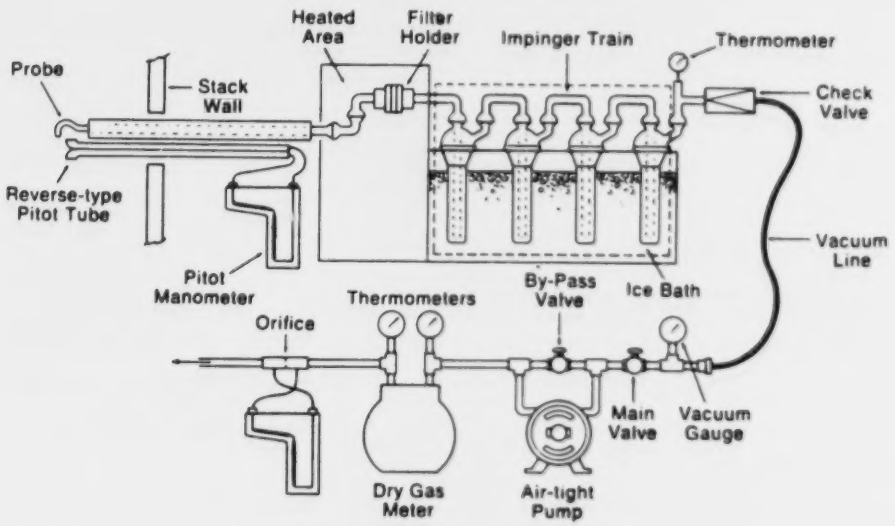

Figure 9. RAC "Staksamplr" schematic of EPA particulate sampling train (Method 5)

Particulate size distribution was determined using an Anderson Mark III high-temperature, multistage, cascade impactor inserted into the RAC sampling train. Data were analyzed by the D_{50} Method. Because of sampling time restrictions, size distribution data could only be taken at the higher char feed rates.

For all particulate trials, the sampling probe assembly was inserted into the stack about 10-stack-diameters downstream of the flue and 3-diameters upstream of the top of the stack. Isokinetic sampling conditions were maintained for all trials to within $\pm$8%, at worst. Sampling times were normally from 1/2 to 1-1/2 hours, depending on the particulate loading rate.

EXPERIMENTAL PLAN

PHASE I. EMISSION LEVELS OF PORTED BAFFLE BURNER

Task 1.0 Base-line Evaluation of NO_x Emissions With Natural Gas

To insure a level of NO_x emissions characteristic of an industrial process furnace and allow an accurate evaluation of changes in process furnace efficiency when retrofitting to a "dirty" off-gas, the pilot-scale industrial test furnace was modified to model an industrial process furnace. The ported baffle burner (PBB) was fired with natural gas, and water-cooling tubes were inserted vertically along the furnace sidewalls until the pilot-scale furnace reached an efficiency typical of industrial practice. This efficiency was determined by a mass energy balance around the furnace; the input data collected for this balance included —

- Temperature profile at the furnace flue using a suction pyrometer
- Detailed flue-gas analysis with a thermal conductivity chromatograph
- Flue-gas velocities with a modified Hubbard probe using an electric manometer
- Inside wall temperatures using an optical pyrometer
- Outside wall temperature with thermocouples
- Water volume through the cooling tubes with a flow meter
- Water inlet/outlet temperatures with thermocouples.

Once the furnace load had been fixed (number and position of cooling tubes) the overall furnace efficiency, flame emissivity, flue-gas concentration measurements, and particulate emissions were measured. The furnace efficiency and NO_x flue concentration measurements were taken throughout the program anytime the fuel or furnace operating conditions were altered.

Task 2.0. NO_x Emissions and Furnace Performance for "Clean" Wellman-Galusha Oxygen Gas

To evaluate the changes in NO_x emission levels and furnace efficiency when retrofitting to a "clean" producer gas, the PBB was fired with "clean" Wellman-Galusha oxygen gas. The two fuel compositions tested during this task are listed in Table 4. To quantify these changes and provide means to correlate the natural gas test results with the "dirty" Wellman-Galusha data, the following subtasks were conducted.

Task 2.1. "Clean" Ambient Temperature Wellman-Galusha Oxygen--

During this subtask, the PBB was fired with "clean" Wellman-Galusha oxygen gas delivered to the burner at ambient temperature. The fuel composition being tested at its delivery temperature was typical of a gasification system that includes a complete post-gasifier cleanup system. The data gathered during this trial (NO_x emissions and furnace efficiency) provided a first line of correlation with the natural gas data.

Task 2.2. "Clean" Hot Wellman-Galusha Oxygen Gas--

The hot "dirty" producer gas that was studied during the program contained ammonia, tar-oils, and char. A base-line test was conducted to establish the changes in NO_x emissions and furnace efficiency that were due to increases in the adiabatic flame temperature and the contributions that were made by the ammonia, tar-oils, and char. This test employed "clean" Wellman-Galusha oxygen gas delivered hot. Data were collected on NO_x emmission levels and overall furnace efficiency.

Task 3.0. NO_x Emissions and Furnace Performance for "Dirty" Wellman-Galusha Oxygen Gas

Hot "dirty" producer gas contains a number of components (ammonia, tar-oils, and char) that were expected to affect NO_x emissions and flame emissivity (resulting in a change in furnace efficiency) as compared with natural gas and/or "clean" producer gas. The following subtasks were designed to evaluate the relative contributions of each of these sources to the total NO_x emission level and quantify any changes in furnace efficiency that resulted from their presence in the gas.

Task 3.1. Addition of Ammonia to "Clean" Hot Wellman-Galusha Oxygen Gas--

To investigate the conversion efficiency dependence on fuel gas ammonia concentration, NO_x emission levels were measured for various concentrations of ammonia in the fuel. The effect of excess air was determined by making the above measurements with 10% and 20% levels of excess air.

As an initial experiment, with 1% ammonia addition, the oxygen in the flue was set to the level required for 10% excess air with the undoped fuel. The ammonia doping level was then reduced in five steps to 0.2% and the NO_x

and O_2 levels were monitored. This experiment showed the effect of the ammonia doping on the oxygen levels in the flue. At high doping levels, it was necessary to include the ammonia as fuel when setting the excess air.

Task 3.2. H_2S Effect on NO_x Emissions From Hot Wellman-Galusha Oxygen Gas Containing Ammonia--

To provide a quantitative answer to the possible interaction of fuel-sulfur and fuel-nitrogen, a hot Wellman-Galusha oxygen gas stream with 1.0% ammonia was doped with different amounts of H_2S.

Task 3.3. Addition of Tar-Oils to "Clean" Hot Wellman-Galusha Oxygen Gas--

Since tar-oils contain chemically bound nitrogen, the purpose of this task was to determine the contribution that they made to NO_x emissions and what effect they had on the overall furnace efficiency.

To permit an evaluation of tar-oils conversion to NO_x, several doping levels were used. Overall furnace efficiencies were measured. The heating value of the tar was included in the fuel enthalpy input.

Task 3.4. Addition of Char to "Clean" Hot Wellman-Galusha Oxygen Gas--

Like tar-oils, char contains fuel-bound nitrogen that could convert to NO_x. To evaluate the percentage conversion of the char-bound nitrogen to NO_x and the dependence of furnace efficiency on fuel char concentration, several levels of char were doped into the gas stream. At each doping level, NO_x emissions, particulate emissions, and furnace efficiency were measured.

Task 3.5. "Dirty" Wellman-Galusha Oxygen Gas--

The purpose of this task was to quantify NO_x and particulate emissions and to evaluate furnace efficiency for the PBB burning "dirty" Wellman-Galusha oxygen gas. "Dirty" Wellman-Galusha oxygen gas was defined for this program as "clean" hot Wellman-Galusha oxygen gas doped with ammonia, char, and tar. This gas was similar in composition to that received from a high-temperature sulfur-removal system.

Task 3.6. Parametric Study of "Dirty" Wellman-Galusha Oxygen Gas--

It was not anticipated that the separate contributions of ammonia, tar-oils, and char to the level of NO_x emissions will equal the concentration

measured for "dirty" Wellman-Galusha oxygen gas. To evaluate the relative contribution of each of these potential sources of NO_x emissions during the combustion of Wellman-Galusha oxygen gas, a number of possible combinations of ammonia, tar-oils, and char were tested. Doping combinations tested included —

- Ammonia/Tar-Oils
- Ammonia/Char
- Char/Tar-Oils.

For each test condition, the NO_x emission level was measured and overall furnace efficiency was evaluated.

Task 3.7. Evaluation of Reduced Emissions Through Combustion Aerodynamics Using Wellman-Galusha Oxygen Gas--

"Dirty" hot Wellman oxygen gas was tested with 15% external flue-gas recirculation to determine the effect on NO_x emissions.

Task 4.0. NO_x Emissions and Furnace Performance for Wellman-Galusha Air Gas

The two controlling factors in NO_x formation and furnace performance, adiabatic flame temperature and combustion aerodynamics, are significantly different between Wellman-Galusha oxygen and air gases. To quantify these differences in NO_x emission levels and furnace efficiency for a "clean" and "dirty" Wellman-Galusha air gas for an industrial PBB, the following subtasks were performed.

Task 4.1. "Clean" Ambient and Hot Wellman-Galusha Air--

This test established a furnace efficiency base line and NO_x emission level for "clean" ambient Wellman-Galusha air gas with the PBB. To evaulate the effect of fuel preheat on emissions and furnace performance, hot Wellman-Galusha air gas was also tested.

Task 4.2. "Dirty" Wellman-Galusha Air--

"Dirty" Wellman-Galusha air gas was fired on the PBB to quantify the level of NO_x emissions and evaluate furnace efficiency.

PHASE II. EMISSION LEVELS OF FUEL MOMENTUM CONTROL BURNER

Phase II of the proposed program was designed to evaluate changes in NO_x emissions and furnace efficiency caused by combustion aerodynamics. During this program phase, tasks identical to those in Phase I were repeated with the fuel momentum control burner (FMCB).

RESULTS

Summaries of all the test data for the ported baffle burner and the fuel momentum controlled burner are presented in Tables 5 and 6 respectively. The following sections present the detailed findings by fuel type.

NATURAL GAS: BASE-LINE TESTS.

Baffle Burner Tests

A baffle burner, representative of the forward-flow type, was the first burner to be utilized. The burner tested, illustrated in Figures 10 and 11, is full scale and is available as an off-the-shelf item from the manufacturer (Bloom Engineering). The burner consists of a centrally located gas nozzle, surrounded by a high-temperature refractory baffle that has ports for the injection of combustion air into the furnace. The flame patterns produced by this burner can be altered by changing the angles of these air ports or their diameters.

This type of burner is found on many large-scale industrial process heating furnaces such as steel reheating, batch glass melting, aluminum holding, and tunnel kilns. The baffle design selected for testing produces a flame-to-furnace length ratio equal to the flame-to-preheat section length ratio found in a five-zone steel slab reheat furnace. Figure 12 illustrates a five-zone steel slab reheating furnace.

More than 60% of the fuel used in a reheat furnace is consumed in the preheat section.

The baffle burner selected for testing was fired at 3.5 million Btu/hr. This fuel input produces a pilot-scale volumetric heat release rate of 12,000 Btu/ft^3-hr, which is within the range (10,000 to 25,000 Btu/ft^3-hr) of industrial firing densities. The baffle used to produce the desired flame-to-furnace length ratio has eight holes, 2.2 inches in diameter, rotated at a 15-degree angle.

The rate of heat absorption and efficiency of the furnace preheat section was simulated on the pilot-scale furnace by inserting water cooling tubes along the furnace sidewalls. A scaled drawing of the test furnace is shown in

TABLE 5. SUMMARY OF TEST DATA FOR BAFFLE BURNER

	Inputs					Flue-Gas Composition (as measured)							Particulate,	
	Rate	NH_3	H_2S	Tar	Char	NO	NO_2	CO	CO_2	O_2	SO_2	HC	g/m^3	g/s
	m^3/s	— % —		— g/s —		— ppm —			— % —		— ppm —			
Fuel Type														
Natural Gas	0.027	0	0	0	0	112	10	10	10.9	1.9	--	--		
WGO* (322K, 10%) Excess Air	0.111	0	0	0	0	38	10	200	24.0	1.8	--	--		
WGO* (700K, 10%) Excess Air	0.140	0	0	0	0	30	5	115	24.0	1.8	--	--		
	0.134	0.19	0	0	0	310	10	55	24.0	1.9	--	--		
	0.134	0.38	0	0	0	360	10	55	24.0	1.8	--	--		
	0.134	0.60	0	0	0	400	15	53	24.0	1.9	--	--		
	0.134	0.81	0	0	0	420	20	55	24.0	1.9	--	--		
	0.134	1.03	0	0	0	430	20	60	24.0	1.9	--	--		
WGO* (700K, 20%) Excess Air	0.134	0	0	0	0	38	5	45	22.0	3.3	--	--		
	0.134	0.19	0	0	0	290	10	45	22.0	3.3	--	--		
	0.134	0.38	0	0	0	355	10	45	22.0	3.2	--	--		
	0.134	0.60	0	0	0	410	20	40	22.0	3.2	--	--		
	0.134	0.81	0	0	0	435	20	40	22.0	3.2	--	--		
	0.134	1.03	0	0	0	465	20	40	22.0	3.3	--	--		
WGO* (700K, 10%) Excess Air Tar Doping	0.141	0	0	0.36	0	52	7	108	24.0	1.8	1	< 1		
	0.141	0	0	0.50	0	55	5	93	24.0	1.9	1	< 1		
	0.141	0	0	0.71	0	58	4	93	24.0	1.9	2	< 1		
WGO* (700K, 10%) Char Doping	0.138	0	0	0	0.13	30	3	59	24.0	1.8	4	< 1	0.037	0.009
	0.138	0	0	0	0.24	33	2	100	24.0	1.7	6	< 1	0.070	0.017
	0.138	0	0	0	0.86	44	4	90	24.0	1.9	29	< 1	0.263	0.064
WGO* (700K, 10%) Ammonia/Tar	0.139	0.99	0	0.39	0	520	10	108	24.0	1.7	2	< 1		
WGO* (700K, 10%) Ammonia/Char	0.138	1.00	0	0	0.13	470	43	65	24.0	1.8	4	< 1		
WGO* (700K, 10%) Char/Tar	0.138	0	0	0.46	0.13	40	8	63	24.0	1.9	7	< 1		
WGO* (700K, 10%) Ammonia/Char/Tar	0.138	1.00	0	0.47	0.13	500	42	75	24.0	1.8	8	< 1		
	0.136	1.02	0	0.38	0.07	510	15	24	24.0	1.9	7	< 1	0.026	0.006
WGO* + 15% FGR (700K, 10%) Ammonia/Char/Tar	0.138	1.00	0	1.22	0.13	510	20	45	24.0	1.9	4	< 1		
WGO* (700K, 10%) Hydrogen Sulfide	0.134	1.04	0.02	0	0	480	29	40	24.0	1.8	83	--		
	0.134	1.04	0.52	0	0	655	33	50	24.0	1.8	2546	--		
	0.136	1.02	2.53	0	0	950	50	37	24.0	1.9	11146	--		
WGA+ (322K, 10% Excess Air)	0.175	0	0	0	0	16	1	260	18.4	1.3	--	--		
WGA+ (616K, 10% Excess Air)	0.175	0	0	0	0	22	2	35	18.4	1.4	--	--		
WGA‡ (616K, 10%) Ammonia/Char/Tar	0.186	1.04	0	0.58	0.35	610	20	40	18.4	1.4	8	< 1	0.044	0.016

* Wellman-Galusha oxygen fuel gas.

\+ Wellman-Galusha air fuel gas.

‡ Wellman-Galusha air fuel gas. Uses 3-inch nozzle. (All others used 2-1/2 inch nozzle.)

TABLE 6. SUMMARY OF TEST DATA FOR KILN BURNER

Fuel Type	Rate[d] m^3/s	Inputs: NH_3 %	Inputs: H_2S %	Inputs: Tar g/s	Inputs: Char g/s	Flue-Gas Composition: NO ppm	NO_2 ppm	CO ppm	CO_2 %	O_2 %	SO_2 ppm	HC ppm	Particulates, g/m^3	Particulates, g/s
Natural Gas[a]	0.027	0	0	0	0	70	5	150	10.2	2.1	—	—	—	—
WGO[a,b] (316 K, 10% Excess Air)	0.104	0	0	0	0	35	5	405	24.0	1.9	—	—	—	—
WGO (705 K, 10% Excess Air)	0.127	0	0	0	0	24	4	34	24.0	1.8	—	—	—	—
	0.127	0.20	0	0	0	270	20	30	24.0	1.8	—	—	—	—
	0.127	0.40	0	0	0	360	30	34	24.0	1.8	—	—	—	—
	0.127	0.63	0	0	0	420	30	32	24.0	1.8	—	—	—	—
	0.127	0.85	0	0	0	460	40	25	24.0	1.8	—	—	—	—
	0.127	1.09	0	0	0	500	40	34	24.0	1.8	—	—	—	—
WGO (705 K, 20% Excess Air)	0.127	0	0	0	0	40	5	25	22.0	3.3	—	—	—	—
	0.127	0.20	0	0	0	270	20	25	22.0	3.3	—	—	—	—
	0.127	0.40	0	0	0	370	30	25	22.0	3.3	—	—	—	—
	0.127	0.63	0	0	0	420	30	25	22.0	3.3	—	—	—	—
	0.127	0.85	0	0	0	480	40	25	22.0	3.3	—	—	—	—
	0.127	1.09	0	0	0	550	50	20	22.0	3.3	—	—	—	—
WGO (705 K, 10% Excess Air) Hydrogen Sulfide	0.127	1.09	0.02	0	0	470	30	34	24.0	1.7	90		—	—
	0.127	1.09	0.54	0	0	700	40	34	24.0	1.7	2579		—	—
	0.127	1.09	2.89	0	0	920	80	34	24.0	1.7	12800	—	—	—
WGO (705 K, 10%) Char Doping	0.124	0	0	0	0.13	30	5	30	24.0	1.8	3	<1	0.037	0.009
	0.127	0	0	0	0.29	35	2	40	24.0	1.9	6	<1	0.050	0.012
	0.134	0	0	0	0.67	55	5	75	24.0	1.7	10	<1	0.129	0.031
WGO (705 K, 10%) Tar Doping	0.136	0	0	0.38	0	50	5	50	24.0	1.8	1	<1	—	—
	0.136	0	0	0.60	0	52	3	57	24.0	1.8	1	<1	—	—
	0.136	0	0	0.73	0	58	4	70	24.0	1.7	2	<1	—	—
WGO (705 K, 10%) Ammonia/Tar	0.129	1.07	0	0.63	0	540	40	75	24.0	1.9	1	<1	—	—
WGO (705 K, 10%) Ammonia/Char	0.144	0.98	0	0	0.13	480	30	33	24.0	1.8	3	<1	—	—
WGO (705 K, 10%) Char/Tar	0.136	0	0	0.48	0.33	65	5	45	24.0	1.9	6	<1	—	—
WGO (705 K, 10%) Ammonia/Char/Tar	0.136	1.02	0	0.25	0.35	540	40	40	24.0	1.8	7	<1	0.065	0.016
WGO + 15% FGR (705 K, 10%) Ammonia/Char/Tar	0.136	1.02	0	0.57	0.13	525	30	50	24.0	1.8	4	<1	—	—
WGA[c] (322 K, 10%) Clean	0.164	0	0	0	0	22	4	200	18.0	1.3	—	—	—	—
WGA (620 K, 10%) Hot/Clean	0.177	0	0	0	0	19	2	30	18.0	1.3	—	—	—	—
WGA (620 K, 10%) Ammonia/Char/Tar	0.172	0.99	0	0.45	0.13	460	30	35	18.0	1.3	7	<1	0.025	0.010

a Used 1-1/2 inch Schedule 10 (axial) fuel injector; all others used 4-inch Schedule 10 injector.

b Wellman-Galusha oxygen fuel gas.

c Wellman-Galusha air fuel gas.

d Fuel flow times heating value adjusted to give from 1.00 to 1.05 MJ/s input.

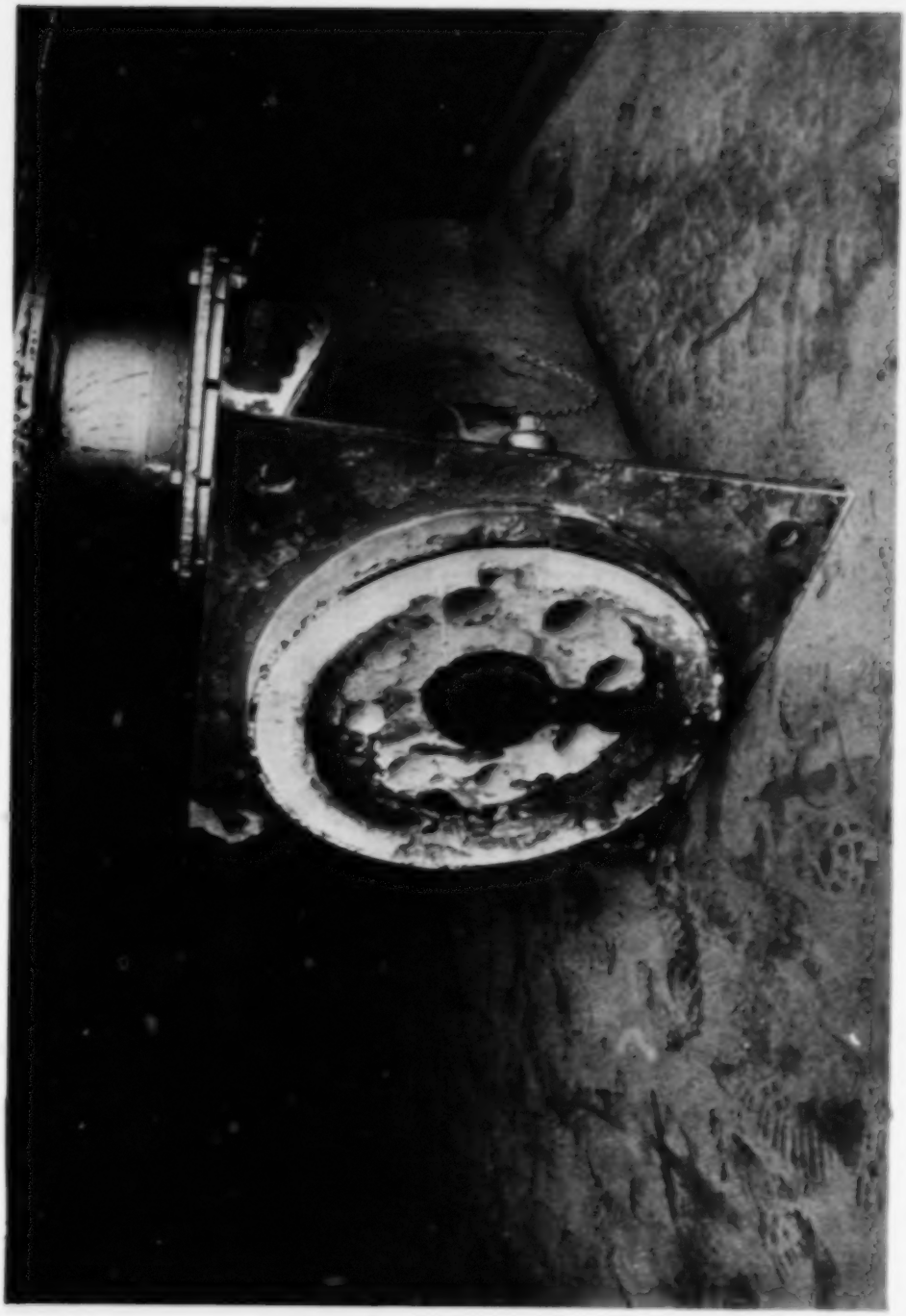

Figure 10. Bloom baffle burner

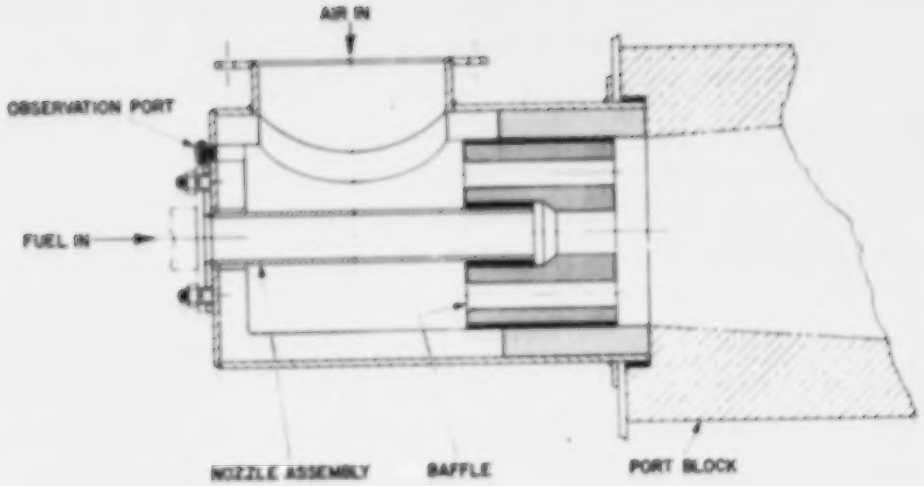

Figure 11. Assembly drawing of baffle burner

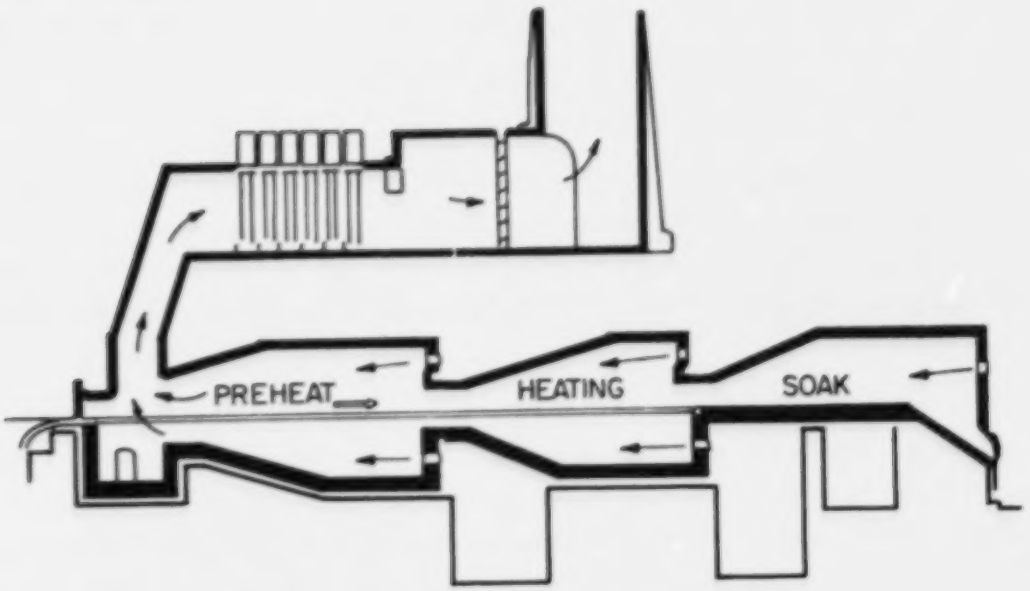

Figure 12. Profile of five-zone reheating furnace with overhead metal recuperator

Figure 13. The locations of the 58 water cooling tubes, which can be placed within the furnace, are indicated by circles. The heat-absorption profile typical of a five-zone reheat furnace preheat section is given in Figure 14. The curve has been plotted in dimensionless units to make scaling easier. In addition to reproducing this heat absorption profile, the furnace should be operated with a thermal load efficiency (heat absorbed by water cooling tubes divided by the fuel input enthalpy)of between 30% and 40%. To achieve an efficiency and heat absorption rate in this range, nine cooling tubes were inserted into the furnace. These tubes are denoted in Figure 13 by the filled-in circles. The heat absorption curve of Figure 14 was reproduced in our furnace by adjusting the cooling surface area of each heat sink. This is accomplished by altering the length of each cooling tube exposed within the furnace. The entire thermal load was placed on the right furnace sidewall, which would simulate the hearth of the reheat furnace. Thus all temperature, radiation, gas compsition, and flow direction profile data represent variations in the vertical plane of the reheat furnace. If the flame were symmetrical about the burner axis, the relative orientation of the test furnace to reheat furnace would not matter. Photographs show that the flame is asymmetrical. Thus, it is important to interpret the results as viewing the combustion process from the roof of a reheat furnace.

Fuel Momentum Controlled Burner Tests

A fuel momentum controlled kiln burner (FMCB) was installed on the pilot-scale test furnace and set up to specifically simulate a cement kiln. The critical operating parameters were 1) a length sufficient to simulate the calcining and reaction zones, 2) the firing density, and 3) the heat absorption profile.

A typical kiln, shown schematically in Figure 15, consists of preheat, calcining, reaction, and cooling zones. The cross-sectional area (20 sq ft) and length (14 ft) of the IGT pilot furnace allow for a near-ideal simulation of the two zones of primary importance: the calcining and reaction zones. It is the heat transfer in these zones that is sensitive to fuel type. In the calcining zone, calcium and magnesium carbonate are decomposed to calcium and magnesium oxide. In the sintering or reaction zone, several complex reactions occur, and among these the oxides combine with SiO_2 to form silicates.

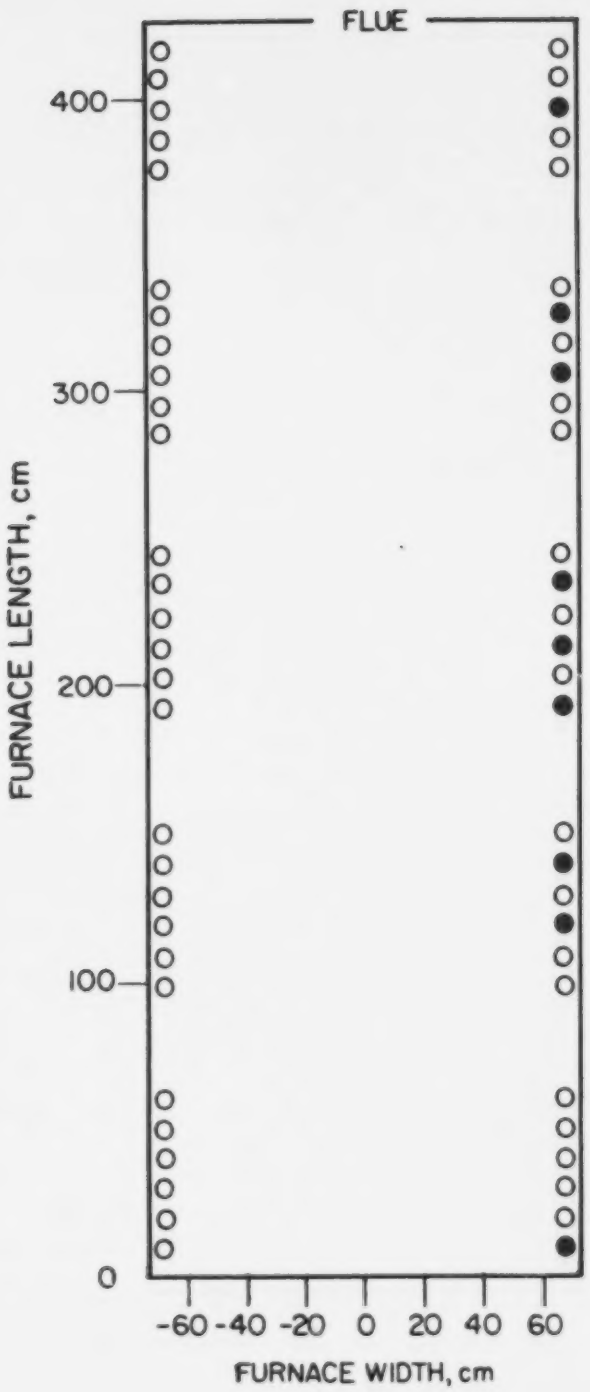

Figure 13. Scaled drawing of test furnace with cooling-tube positions for PBB simulation

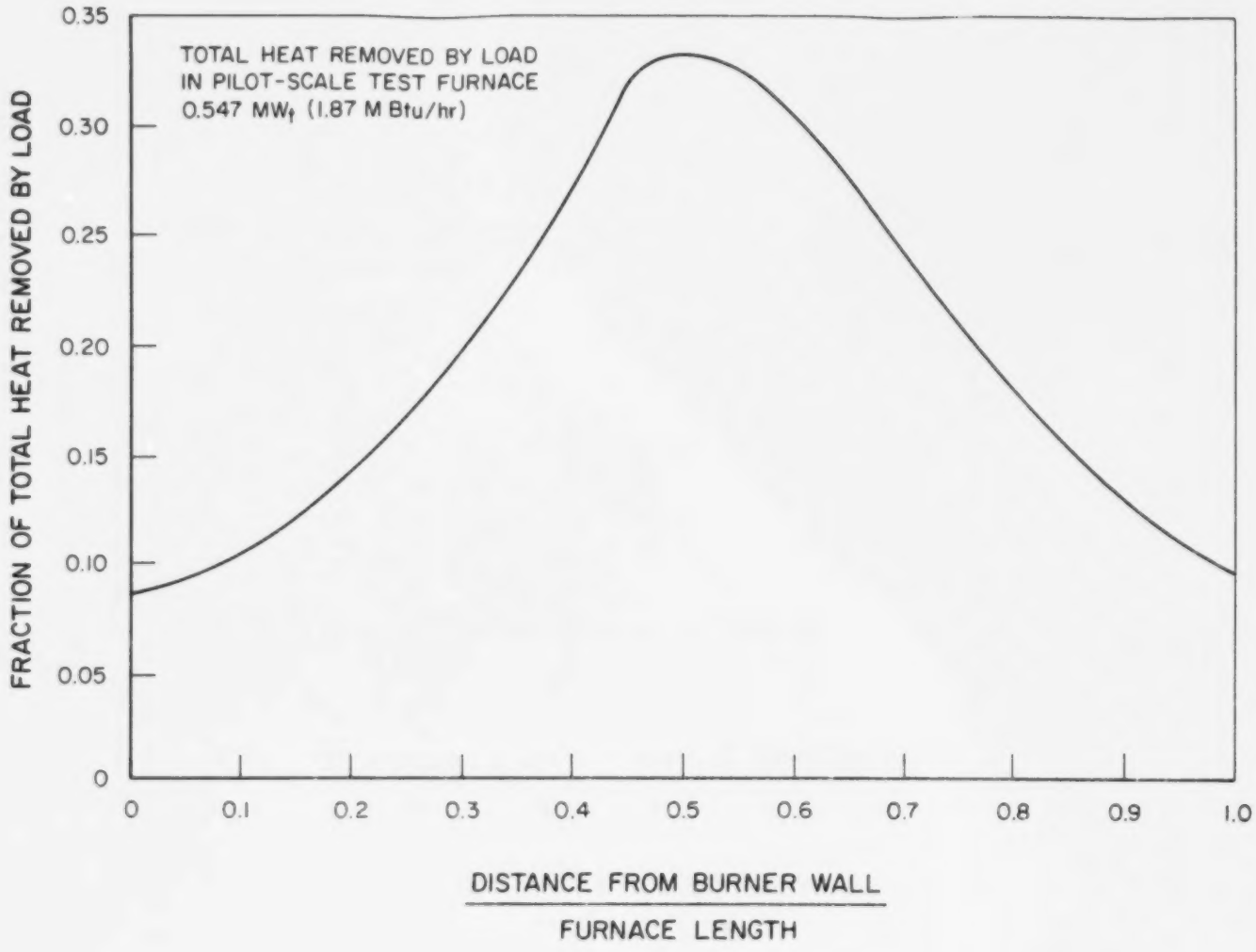

Figure 14. Heat-absorption profile of preheat section of a five-zone reheat furnace as a function of furnace length

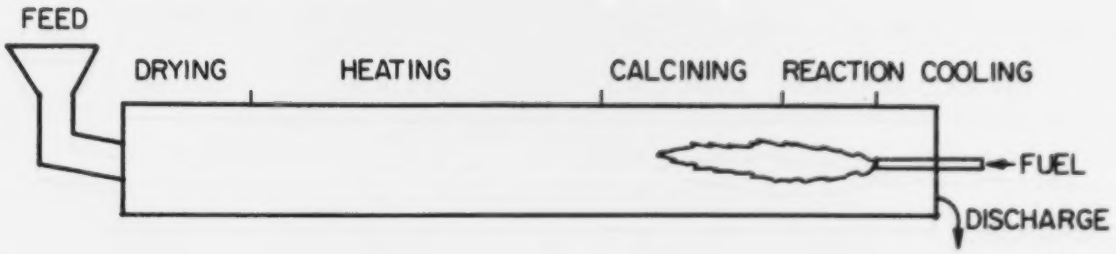

Figure 15. Schematic drawing of a rotary cement kiln

These two zones occupy about one-third of the overall kiln length, with the calcining zone being twice the length of the sintering zone. The flame usually extends three-quarters of the length of these zones.

Firing densities in rotary kilns range from 10,000 to 20,000 Btu/hr-ft^3. A firing density value of 12,500 Btu/hr-ft^3 was used for these tests and is typical of many kilns. This requires a firing rate of 3.5 million Btu/hr for our test furnace volume. Cement kilns require about 5 to 7 million Btu/ton of clinker. Assuming 6 million Btu/hr, our furnace would simulate a production rate of 1150 lb/hr.

In order to determine the heat absorption profile, we must consider the temperature variation of the solid material (clinker) in the kiln. Figure 16

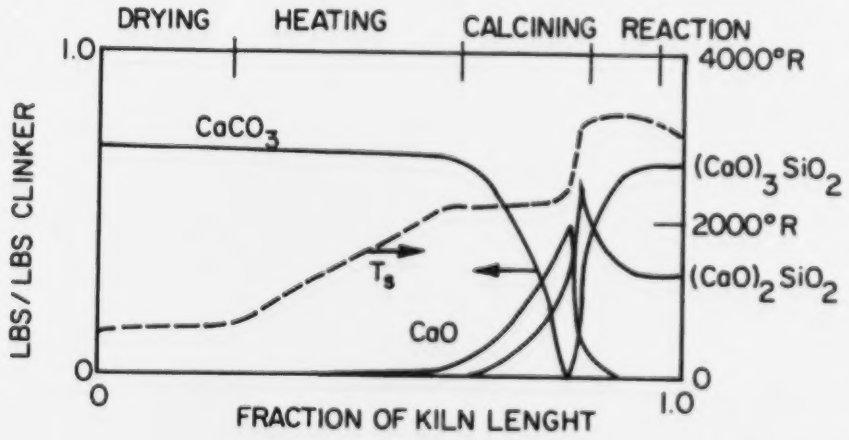

Figure 16. Temperature and composition in a typical cement kiln

shows a typical plot for this temperature. This plot shows that the clinker temperature is relatively constant through the calcining zone and then rises rapidly as it enters the reaction zone. In the calcining zone, calcium and magnesium carbonate decompose by an endothermic reaction to calcium and magnesium oxide;

$$CaCO_3 = CaO + CO_2 \quad -1350 \text{ Btu/lb CaO}$$
$$MgCO_3 = MgO + CO_2 \quad -1264 \text{ Btu/lb MgO}$$

With a composition of about 68% CaO and 1.5% MgO, the heat requirement in the calcining zone is 950 Btu/lb of clinker produced. Therefore, the thermal load in the IGT furnace for the calcining section must be 950 Btu/lb times the 1150 lb/hr simulated production rate or 1.1 million Btu/hr, absorbed relatively uniformly throughout the section.

In the reaction zone, the temperature of the solid (clinker) materials increases rapidly by about 900°F because of the completion of the calcining reactions and the onset of the exothermic reactions. The overall effect is exothermic, releasing approximately 200 Btu/lb of clinker produced, which is equivalent to 230,000 Btu/hr on the IGT test furnace. The increase in the temperature of the materials requires 233,000 Btu/hr (1150 lb/hr X 0.225 Btu/lb-°F X 900°F), so virtually no heat is transferred by the flame in this zone.

Figure 17 shows the required heat-absorption profile. The flame length should be about 10.5 ft, and the total thermal loading of the furnace should be 1.1 million Btu/hr.

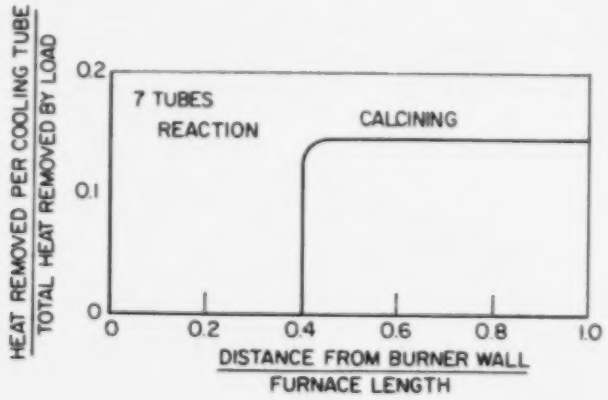

Figure 17. Heat absorption profile of reaction and calcining zones of a rotary cement kiln

This rate of heat absorption and this efficiency were simulated on the pilot-scale furnace by inserting water cooling tubes along the furnace sidewalls, while firing natural gas at 3.5 million Btu/hr. A scaled drawing of the test furnace is shown in Figure 18. The locations of the 58 water-cooling tubes, which can be placed within the furnace, are indicated by circles. The seven filled circles indicate those tubes inserted into the furnace to simulate the desired efficiency and heat absorption rate for the kiln furnace. Figure 19 is a schematic of the kiln burner fuel injector.

WELLMAN-GALUSHA OXYGEN: EMISSION STUDIES

Prior to the doping studies, base-line emissions were obtained for natural gas and Wellman-Galusha oxygen (WGO) fuel gas on the baffle burner and kiln burner and are shown in Table 7. Both fuels were fired at 1.03 ± 0.07 MW_t ($3.50 \pm 0.25 \times 10^6$ Btu/hr) with 10% excess air. The above variation in fuel heat input represents the range of firing rates from run to run and not the firing rate fluctuation during a given run, which was minimal. For all tests the furnace was at positive pressure. All concentrations presented are dry analyses at the flue entrance. For NO_x levels under 100 ppm the reproducibility of the reported values was $\pm$ 5 ppm while at the higher levels it was $\pm$ 10 ppm. Recent studies[11] have shown that quenching may cause interference in NO_x measurements. Our results, however, have not been compensated for such effects.

With natural gas and WGO on the baffle burner a 0.063-m inside diameter (ID) (nominal 2-1/2 inch Schedule 40) fuel nozzle was used. Fuel velocities at the nozzle exit were 40 m/s (130 ft/s, ambient WGO) and 110 m/s (360 ft/s, hot WGO). Natural gas velocity was 9.5 m/s (28 ft/s). Combustion air entered the furnace at velocities of 19 m/s (63 ft/s) for the low-Btu fuels and 23 m/s (76 ft/s) for natural gas.

On the kiln burner a 0.043-m ID (nominal 1-1/2 inch Schedule 10) axial fuel nozzle with a 0.019-m ID (7/8 inch, 16 gauge) tube as the radial injector was employed for natural gas and ambient (322 K) WGO. For hot (700 K) WGO a 0.108-m ID (nominal 4 inch Schedule 10) axial fuel nozzle with a 0.064-m (nominal 2-1/2 inch Schedule 10) radial injector was required to achieve comparable fuel velocities as well as to maintain flame stability. The amount of radial flow for natural gas on the kiln burner was 95% of the total. This

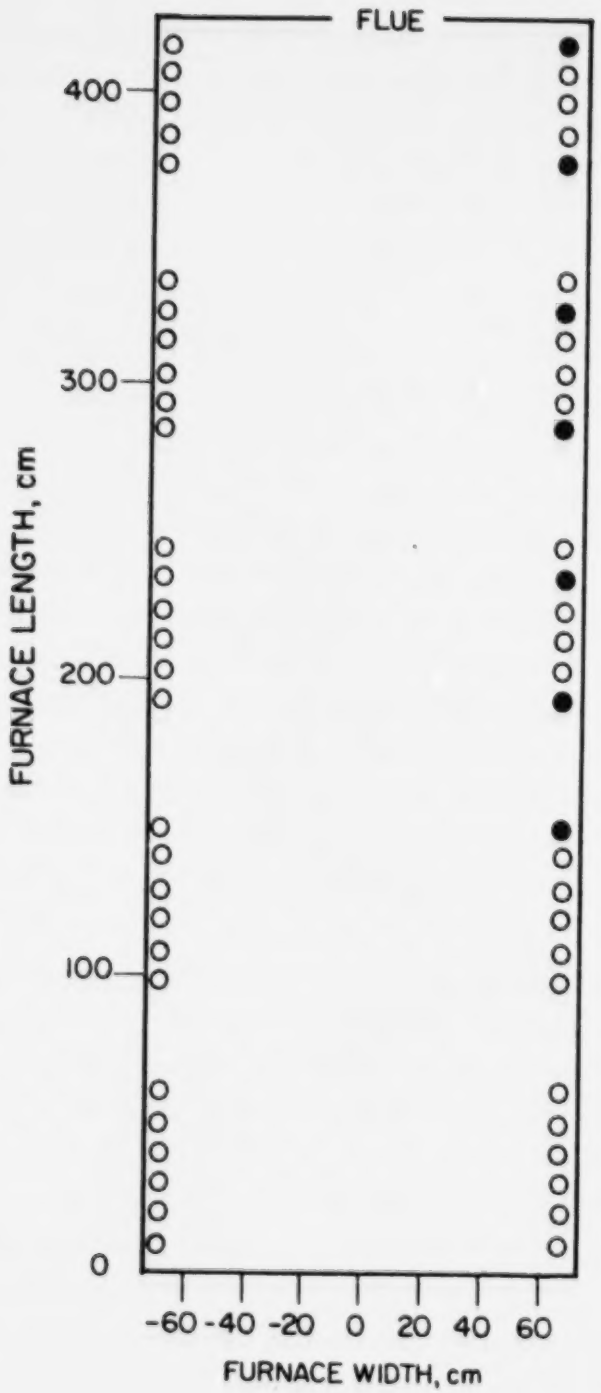

Figure 18. Scaled drawing of test furnace with cooling tube positions for FMCB simulation

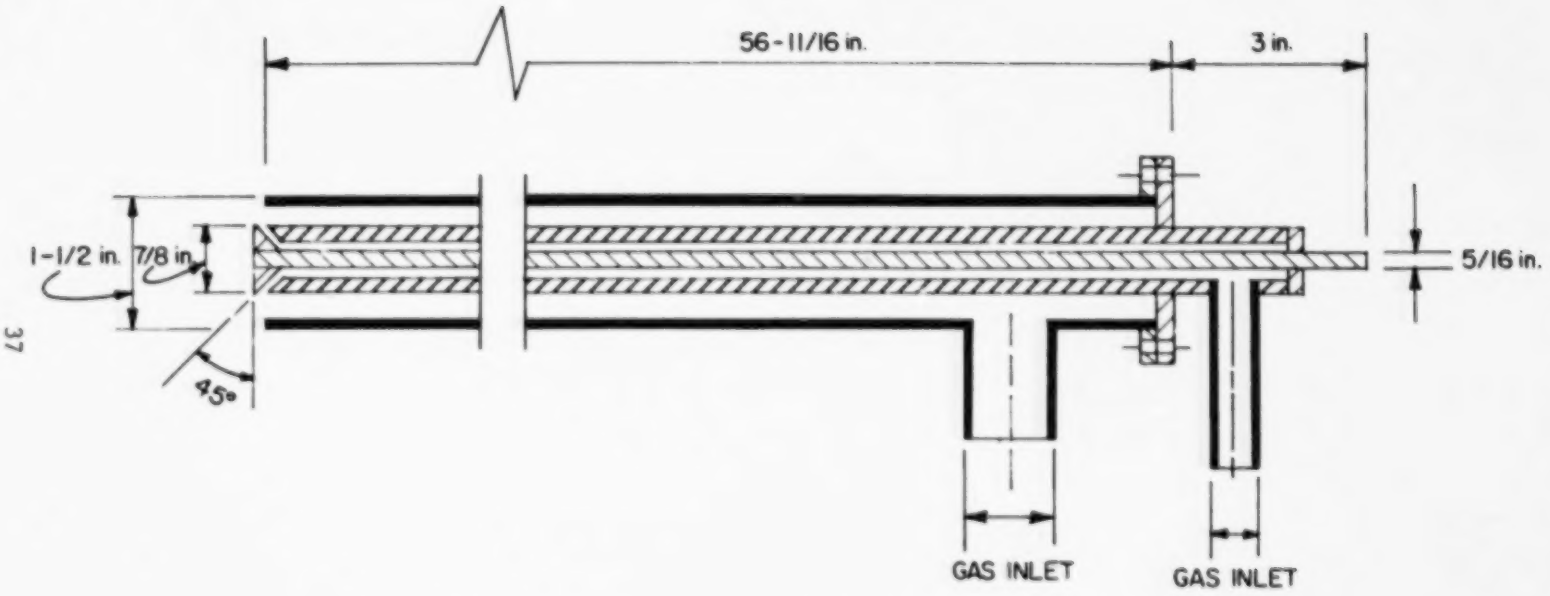

Figure 19. Schematic diagram of the kiln burner fuel injector

TABLE 7. BASE-LINE DATA FOR CLEAN FUELS: NATURAL GAS AND WELLMAN-GALUSHA OXYGEN (WGO), 3.5 MILLION Btu/hr WITH 10% EXCESS AIR

	Fuel Type	Fuel Temperature, K	NO_x* ppm	CO ppm
Baffle Burner	Natural Gas	298	135	10
	WGO	322	53	200
	WGO	700	38	115
Kiln Burner	Natural Gas	298	83	150
	WGO	322	44	405
	WGO	700	31	34

* NO plus NO_2 (Dry, corrected to 0% excess air).

value was selected to give a stable flame of a size compatible with the furnace dimensions. For both ambient and hot WGO the flow was 22% radial, chosen to give a flame length comparable to that of natural gas. With the fuels studied, gas injected radially was at sonic velocity while the axial component entered at 85 m/s (280 ft/s) for ambient WGO. The axial velocity was 52 m/s (170 ft/s) for hot WGO on the larger nozzle. With natural gas the axial flow was 1.2 m/s (4 ft/s). Air velocity with the kiln burner was 3.1 m/s (10 ft/s).

In order to determine the effects of the various potential sources of fuel-NO_x on the measured NO_x levels, char, tar, and ammonia were individually doped into hot WGO. The doping system and the char (0.66 weight percent nitrogen) and tar (0.55 weight percent nitrogen) analyses were presented in the preceeding section. The results of the char and tar doping trials are presented in Tables 8 and 9. For char, the doping rate varied from 0.13 to 0.86 g/s or 0.4 to 2.7 grains/SCF, while the tar levels of 0.36 to 0.73 g/s correspond to 1.1 to 2.3 grains/SCF. The total NO_x levels measured for char or tar are comparable and show a NO_x increase from 0 to 30 ppm. The fact that bound sulfur in the tar (0.47 weight percent sulfur) and char (1.64 weight percent sulfur) is converted to sulfur oxides is evidenced by the SO_2 levels. Increases in NO_x levels above undoped thermal NO_x levels cannot simply be ascribed to fuel-nitrogen conversion when fuel-sulfur is also present. Work of IGT(unpublished) and others[18] has shown that in turbulent diffusion flames thermal NO_x, as well as fuel NO_x, is enhanced by fuel-sulfur. In the tar doping studies the problem of char-like residue collecting inside the fuel nozzle was encountered. On the baffle burner this residue amounted to about 3% by weight of the doped tar, whereas on the kiln burner the residue was around 7% of the tar input.

The effects of various levels of fuel-nitrogen, in the form of ammonia, on the conversion of fuel-nitrogen to NO_x are shown in Tables 10 and 11 and Figures 20 and 21 for the baffle and kiln burners with 10% excess air. Ammonia was metered into the hot WGO at levels of 0.02 to 1.00 volume percent of fuel input. The oxygen level at the flue was maintained at $1.8 \pm 0.1\%$ (dry analysis), corresponding to 10% excess air. The fraction of ammonia converted to NO_x decreases as the fraction of ammonia in the fuel increases. The results are comparable for both burners with the kiln burner giving a somewhat higher conversion.

TABLE 8. CHAR DOPING:
WELLMAN-GALUSHA OXYGEN (700 K),
3.5 MILLION Btu/hr WITH 10% EXCESS AIR

	Char Input, g/s	NO_x*	CO ppm	SO_2
Baffle	0	38	115	0
Burner	0.13	36	59	4
	0.24	38	100	6
	0.86	53	90	29
Kiln	0	31	34	0
Burner	0.13	38	30	3
	0.29	41	40	6
	0.67	66	75	10

* NO plus NO_2 (Dry, corrected to 0% excess air).

TABLE 9. TAR DOPING:
WELLMAN-GALUSHA OXYGEN (700 K),
3.5 MILLION Btu/hr WITH 10% EXCESS AIR

	Tar Input, g/s	NO_x* ppm	CO ppm	SO_2 ppm
Baffle	0	38	115	0
Burner	0.36	65	108	1
	0.50	66	93	1
	0.71	68	93	2
Kiln	0	31	34	0
Burner	0.38	60	50	1
	0.60	60	57	1
	0.73	68	70	2

* NO plus NO_2 (Dry, corrected to 0% excess air).

TABLE 10. AMMONIA CONVERSION TO NO_x ON THE BAFFLE BURNER

NH_3, % in fuel	Excess Air, %	Fuel NO_x,* ppm	NH_3 Conversion, %
0.02	10	77	52
0.11	10	213	29
0.19	10	312	26
0.38	10	367	15
0.60	10	416	11
0.81	10	443	9
1.03	10	454	7
1.42	10	509	6
0.19	20	305	26
0.38	20	382	16
0.60	20	459	13
0.81	20	489	10
1.03	20	524	8

* Dry, corrected to 0% excess air.

TABLE 11. AMMONIA CONVERSION TO NO_x ON THE KILN BURNER

NH_3, % in fuel	Excess Air, %	Fuel NO_x*, ppm	NH_3 Conversion, %
0.03	10	123	60
0.10	10	243	38
0.20	10	287	23
0.40	10	396	16
0.63	10	462	12
0.85	10	516	10
1.09	10	560	8
0.20	20	291	23
0.40	20	421	17
0.63	20	480	12
0.85	20	563	11
1.09	20	658	10

* Dry, corrected to 0% excess air.

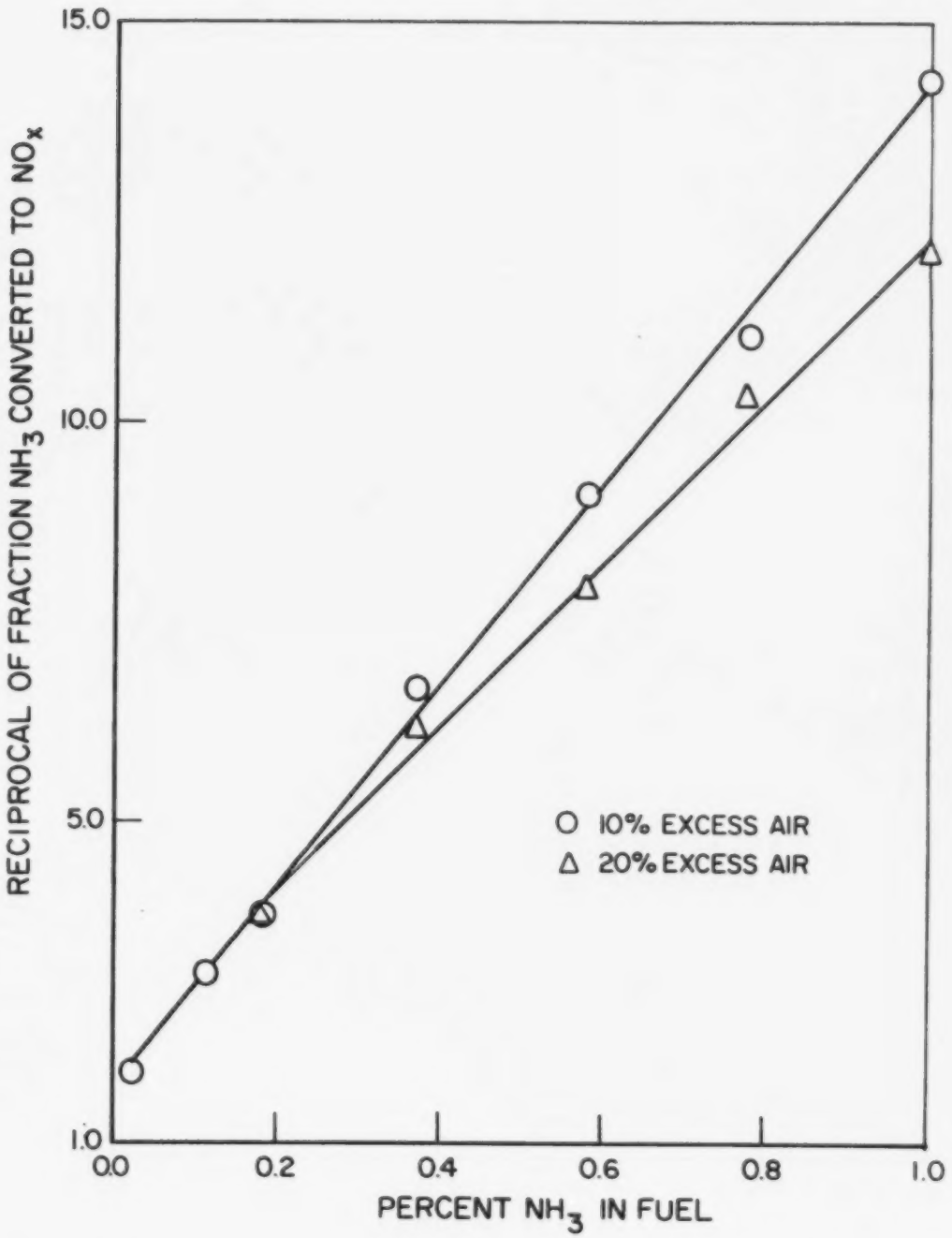

Figure 20. Ammonia conversion for Wellman-Galusha oxygen fuel gas on the baffle burner with 10% and 20% excess air

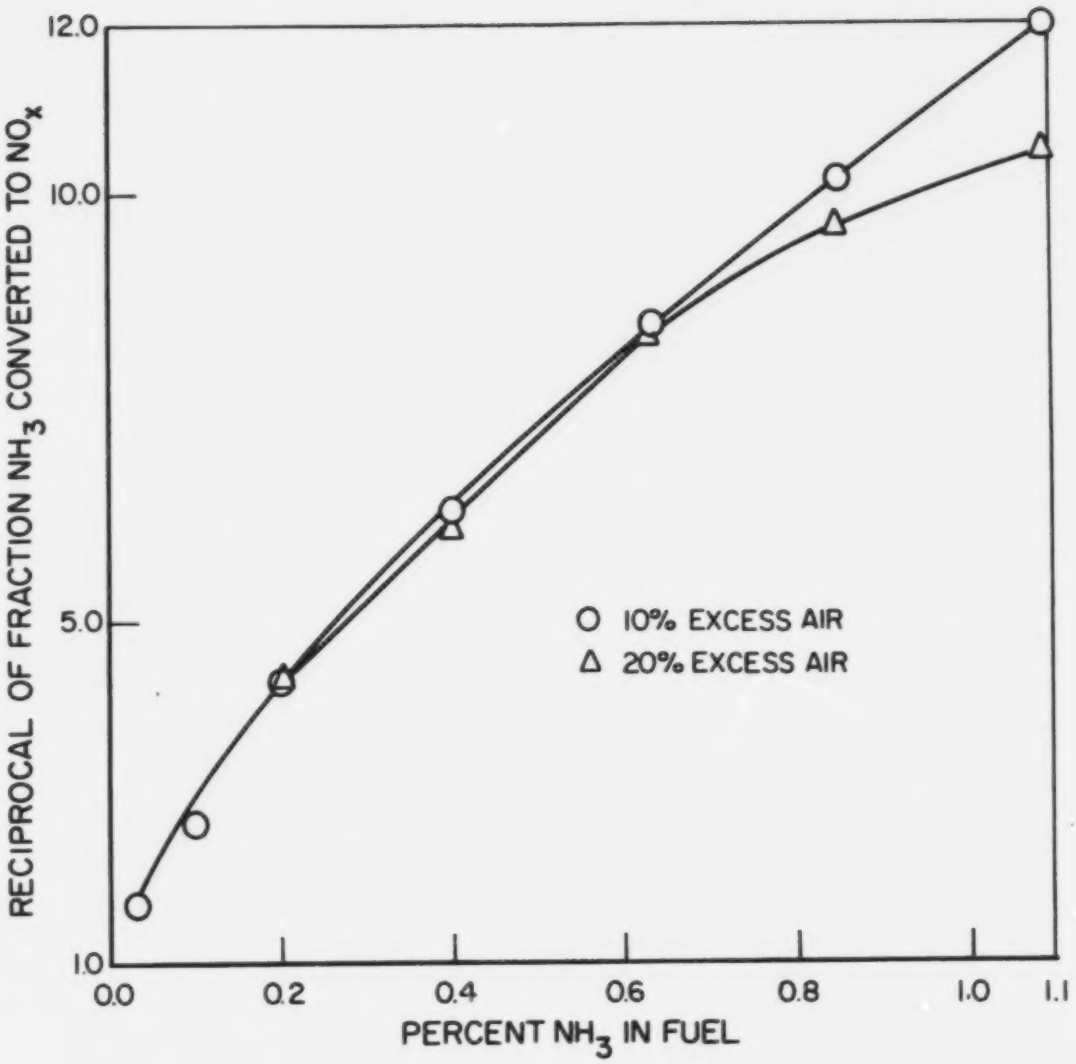

Figure 21. Ammonia conversion for Wellman-Galusha oxygen fuel gas on the kiln burner with 10% and 20% excess air

The effects of changing the amount of excess combustion air are also shown in Tables 10 and 11 and in Figures 20 and 21 for the baffle and kiln burners with 20% excess air. Here, ammonia constituted from 0.20 to 1.09 volume percent of the fuel input. The oxygen level at the flue was held at 3.3 $\pm$ 0.1% (dry analysis) to keep the excess air level at 20%. A comparison of Figures 20 and 21 shows that the fraction of ammonia converted to NO_x increases with an increase in the availability of oxygen. Again the kiln burner gives a slightly higher ammonia-to-NO_x conversion than the baffle burner.

The effects of ammonia doping on flue oxygen levels were determined by setting the flue oxygen to the level required for 10% excess air with 1.0% ammonia addition and then reducing the ammonia level in five steps to 0.2%. For a given reduction of ammonia the oxygen level rose by an amount consistent with the reaction —

$$NH_3 + (0.75 + \frac{f}{2})O_2 = f\ NO + (\frac{1 - f}{2})N_2 + 1.5\ H_2O$$

where f is the fraction of ammonia converted to NO_x.

Since raw hot gasifier effluents contain both fuel-nitrogen and fuel-sulfur the effects of the latter on fuel-nitrogen conversion to NO_x were determined by adding various levels of hydrogen sulfide to 1.0% ammonia-doped hot WGO. The results for both burners are shown on Figure 22. Hydrogen sulfide was metered in from 0.02 to 2.89 volume percent of fuel input. Oxygen in the flue was kept at 1.8%, corresponding to the 10% excess air level. As can be seen, small amounts of fuel-sulfur significantly enhanced fuel-nitrogen conversion to NO_x. Above about 1.5%, and up to 2.9%, hydrogen sulfide did not add greatly to further total NO_x enhancement. These results were essentially the same for both burners.

A review of the literature[1] indicated that the degree of initial fuel/air mixedness had an appreciable effect on fuel-nitrogen conversion to NO_x. With 1.0% ammonia-doped hot WGO at an excess air level held at 10% on the kiln burner, the amount of radial flow was varied from 0 to 36% of the total. The results, shown in Figure 23, confirmed the effect of initial mixing on fuel-NO_x emissions. The ammonia conversion to NO_x rose sharply from 10% radial flow to 36%. The thermal NO_x was not appreciably affected over the same range.

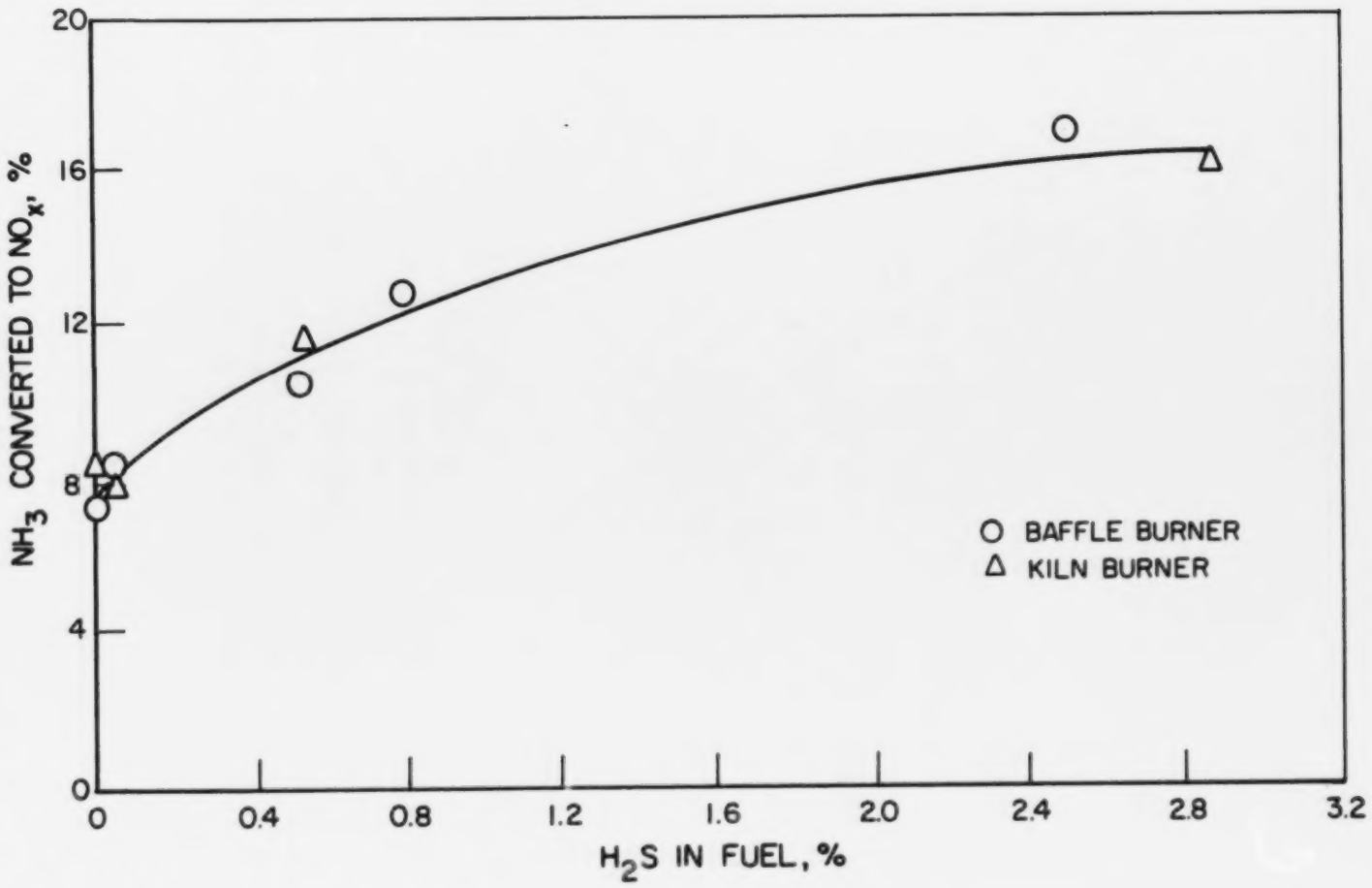

Figure 22. Effect of H_2S on ammonia (1.0% by volume) conversion to NO_x with Wellman-Galusha oxygen (10% excess air)

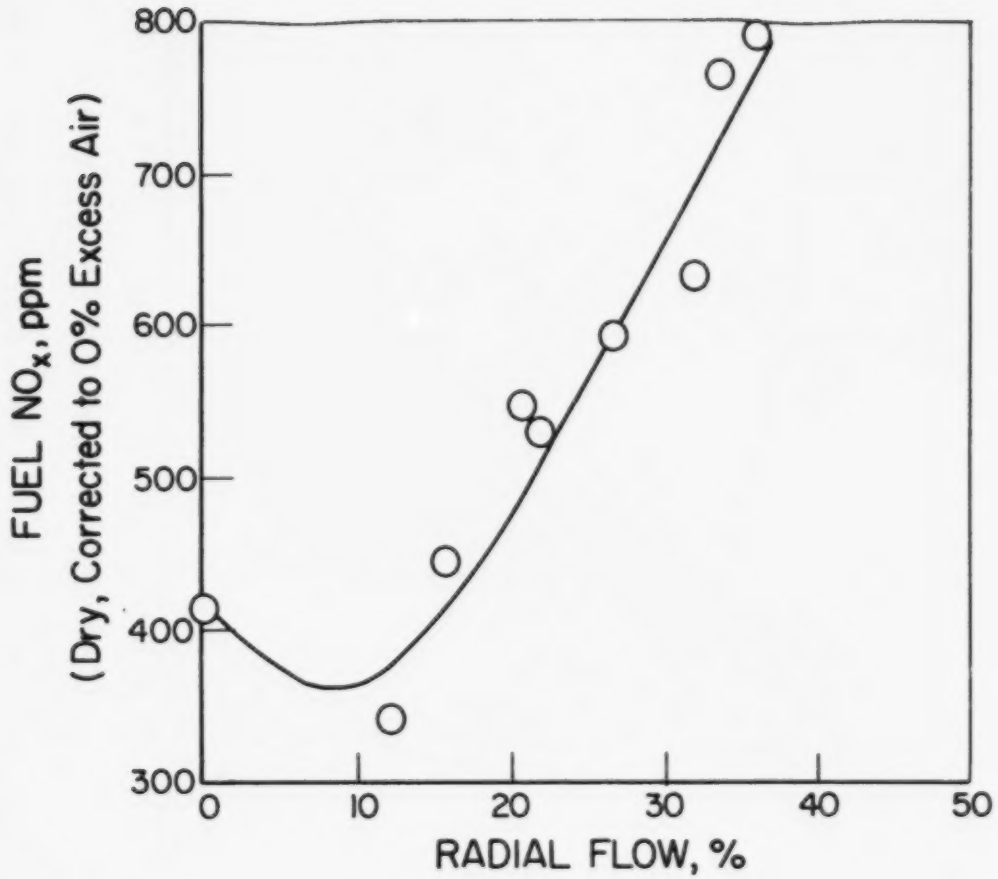

Figure 23. Effects of radial vs. axial flow on ammonia (1.0%) conversion to NO_x with Wellman-Galusha oxygen fuel gas on the kiln burner

Following the single-dopant tests, so-called parametric studies were performed, wherein the various contaminants were added in combinations of two. The results of the ammonia-plus-tar and ammonia-plus-char parametric trials are presented in Table 12. The doping rates were representative of those used in the single-dopant tests. The total NO_x levels were found to be about 5% to 20% higher than expected on a simple additive basis (derived from the single-dopant studies), indicating some kind of synergistic effect.

The char-plus-tar parametric and the ammonia-plus-char-plus-tar ("dirty") doping results are shown in Table 13. Doping levels were again consistent with previous tests, and excess air was held at 10%. Total NO_x levels in the case of char-plus-tar appear to be purely additive while the results of the "dirty" doping trials show the same kind of NO_x enhancement as seen in the ammonia-plus-char and ammonia-plus-tar tests. Total fuel-nitrogen conversion to NO_x is slightly higher on the kiln burner than on the baffle burner ($\sim$10% versus $\sim$9%) if one assumes that thermal NO_x levels are not greatly affected by the sulfur in the dopants.

WELLMAN-GALUSHA AIR: EMISSION STUDIES

As with Wellman-Galusha oxygen (WGO) fuel gas, base-line data were obtained for clean Wellman-Galusha air (WGA) fuel gas at ambient and elevated temperatures on both the baffle and kiln burners. These data are presented in Table 14 along with the base-line natural gas data previously shown in Table 7. The fuels were fired at 1.03 ± 0.07 MW_t ($3.50 \pm 0.25 \times 10^6$ Btu/hr) with 10% excess air. For the baffle burner, natural gas and ambient (322 K) WGA were burned on the same 0.063-m ID (nominal 2-1/2 inch) fuel nozzle as WGO. Hot (616 K) WGA required a 0.078 m ID (nominal 3 inch Schedule 40) fuel nozzle to overcome the stability problems encountered on the 0.063-m ID nozzel. WGA fuel velocities were 63 m/s (206 ft/s) for ambient WGA and 83 m/s (273 ft/s) for hot WGA with combustion air at 19 and 30 m/s (62 and 99 ft/s), respectively.

On the kiln burner, the 0.108-m ID (nominal 4 inch) axial fuel nozzle was used for both ambient and hot WGA. The amount of radial flow was selected to give flame lengths comparable to that of natural gas; ambient WGA was fired with 10% radial flow, while hot WGA required 16% radial flow. Radial gas

TABLE 12. PARAMETRIC DOPING: WELLMAN-GALUSHA OXYGEN (700 K), 3.5 MILLION Btu/hr WITH 10% EXCESS AIR

	Inputs					
	NH_3, vol %	Tar, g/s	Char, g/s	NO_x*	CO, ppm	SO_2
Baffle Burner	0	0	0	38	115	0
	1.03	0	0	492	60	0
	0.99	0.39	0	580	108	2
	1.00	0	0.13	561	65	7
Kiln Burner	0	0	0	31	34	0
	1.09	0	0	591	34	0
	1.07	0.63	0	635	75	1
	0.98	0	0.13	558	33	3

* NO plus NO_2 (Dry, corrected to 0% excess air).

TABLE 13. PARAMETRIC AND "DIRTY" DOPING: WELLM'N-GALUSHA OXYGEN (700 K), 3.5 MILLION Btu/hr WITH 10% EXCESS AIR

	Inputs					
	NH_3, vol %	Tar	Char	NO_x*	CO	SO_2
		g/s		ppm		
Baffle	0	0	0	38	115	0
Burner	1.03	0	0	492	60	0
	0	0.46	0.13	53	63	7
	1.00	0.47	0.13	593	75	8
Kiln	0	0	0	31	34	0
Burner	1.09	0	0	591	34	0
	0	0.48	0.35	77	45	6
	1.02	0.25	0.35	635	40	7

* NO plus NO_2 (Dry, corrected to 0% excess air).

TABLE 14. BASE-LINE DATA FOR CLEAN FUELS: NATURAL GAS AND WELLMAN-GALUSHA AIR (WGA), 3.5 MILLION Btu/hr WITH 10% EXCESS AIR

	Fuel Type	Fuel Temperature, K	NO_x* ppm	CO
Baffle Burner	Natural Gas	298	135	10
	WGA	322	18	260
	WGA	616	26	35
Kiln Burner	Natural Gas	298	83	150
	WGA	322	28	200
	WGA	616	22	30

* NO plus NO_2 (Dry, corrected to 0% excess air).

velocities were sonic while axial fuel velocities varied from 33 m/s (107 ft/s) for ambient WGA to 74 m/s (244 ft/s) for hot WGA. Air velocity was 3.1 m/s (10 ft/s).

Only "dirty" doped, hot WGA was studied. The results are shown in Table 15. If the additives did not greatly affect thermal NO_x levels then the baffle burner is somewhat more efficient in converting fuel-nitrogen to NO_x than the kiln burner, namely, ∿11% versus ∿9%, respectively. This is opposite to the WGO results, where the kiln burner appeared to be slightly more efficient, in converting fuel nitrogen.

PARTICULATE STUDIES

Besides measuring the effects of the various dopants on gas-phase pollutants, total particulates in the stack were measured as well. The instrumentation and sampling technique used were described in a preceding section. Results of these total stack-particulate measurements are presented in Figure 24 for both WGO and WGA on the baffle and kiln burners. The fraction of char-derived particulates surviving in the stack increased from ∿5% at a char input of 0.02 g/s to ∿11% at a char input rate of 1.1 g/s. At all char doping rates, it was visually noted that a qualitatively large number of glowing particles were deposited on the furnace hearth. The presence of ammonia and/or tar did not affect the measured total stack-particulates from char.

In addition to total particulates, particle size distributions were measured for char-doped WGO on the baffle and kiln burners using a cascade impactor and methods described previously. The results are shown in Tables 16 and 17. On the baffle burner, with a char doping rate of 1.14 g/s, 63% of the particles are smaller than roughly 0.7μ, while on the kiln burner, for a char rate of 0.76 g/s, only about 5% of the particles are below 0.7μ. This shift in particle size depends more on char input level than on burner type for the cases here studied. This conclusion is supported by the data obtained from the total particulate measurements wherein an increase in "coarse" particles trapped in the cyclone preseparator relative to "fine" particles staining the filter was observed with decreasing char doping rate for both burners.

TABLE 15. "DIRTY" DOPING:
WELLMAN-GALUSHA AIR (616 K),
3.5 MILLION Btu/hr WITH 10% EXCESS AIR

	Inputs					
	NH_3, %	Tar	Char	NO_x*	CO	SO_2
		g/s		ppm		
Baffle Burner	0	0	0	26	35	0
	1.04	0.58	0.35	672	40	8
Kiln Burner	0	0	0	22	30	0
	0.99	0.45	0.13	522	35	7

* NO plus NO_2 (Dry, corrected to 0% excess air).

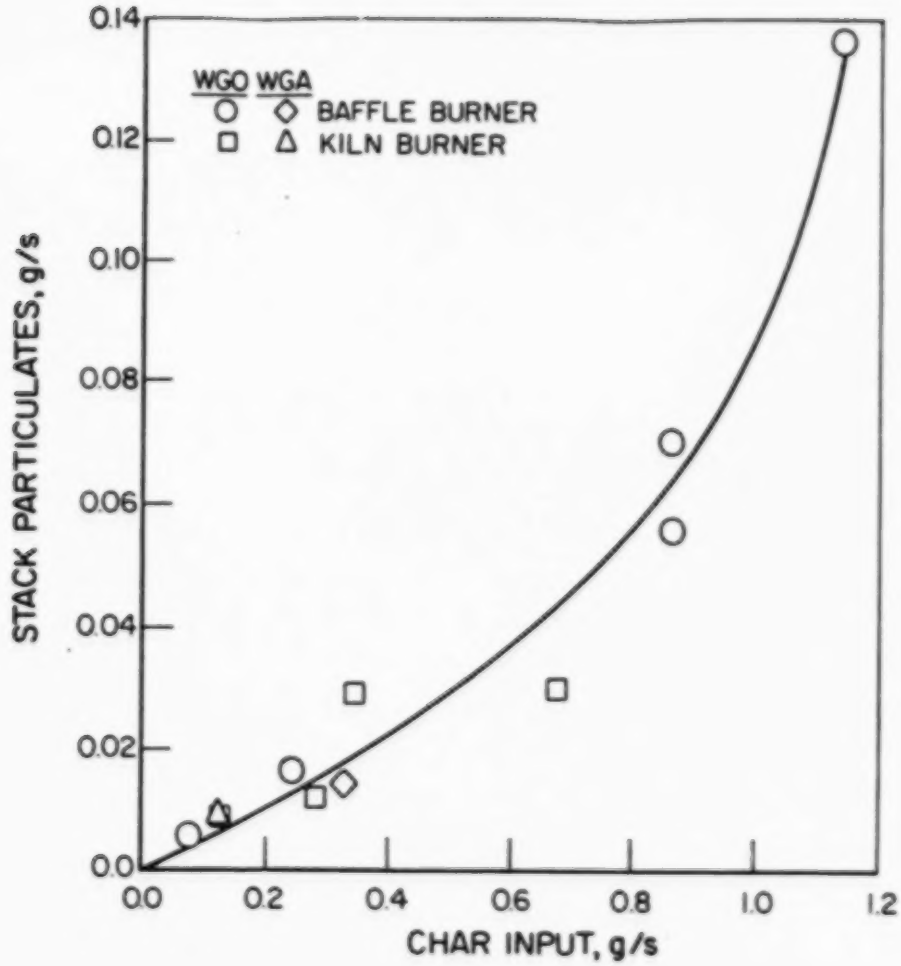

Figure 24. Particulate emissions for char doping of Wellman-Galusha fuel gases on the baffle and kiln burners (10% excess air)

TABLE 16. BAFFLE BURNER CASCADE IMPACTOR
RESULTS FOR CHAR-DOPED WELLMAN-GALUSHA OXYGEN (700 K)—
DOPING RATE: 1.14 g/s

Stage	Size (μ)	Wt %	% Cumulative*
0	≥17.1	11.1	88.9
1	10.7 - 17.1	1.4	87.5
2	7.3 - 10.1	0.4	87.1
3	5.0 - 7.3	2.9	84.2
4	3.2 - 5.0	2.5	81.7
5	1.8 - 3.2	8.9	72.8
6	1.1 - 1.8	4.7	68.1
7	0.7 - 1.1	5.6	62.5
Filter	0 - 0.7	62.5	0

* Wt % of particulates passing through stage.

TABLE 17. KILN BURNER CASCADE IMPACTOR
RESULTS FOR CHAR-DOPED WELLMAN-GALUSHA OXYGEN (700 K)—
DOPING RATE: 0.76 g/s

Stage	Size (μ)	Wt %	% Cumulative*
0	≥12.6	48.5	51.5
1	7.9 - 12.6	4.9	46.6
2	5.3 - 7.9	9.2	37.4
3	3.6 - 5.3	7.2	30.2
4	2.4 - 3.6	5.8	24.4
5	1.2 - 2.4	12.1	12.3
6	0.7 - 1.2	7.8	4.5
7	0.5 - 0.7	0.2	4.3
Filter	0 - 0.5	4.3	0

* Wt % of particulates passing through stage.

FURNACE EFFICIENCY

Aside from the pollution aspects of burning low-Btu fuel gases as substitutes for natural gas, potential users of low-Btu gas are also very interested in retrofitting problems that might be encountered. One phase of any retrofit evaluation is the effect of firing low-Btu gas on furnace efficiency and heat transfer to the load. As noted in an earlier section, water-cooling tubes were positioned along the furnace wall to simulate the load of a steel reheat furnace for use with the baffle burner and then to simulate the calcining and reaction zones of a cement kiln for use with the kiln burner.

For the baffle burners, fired at 1.03 MW_t (3.5 X 10^6 Btu/hr), furnace thermal efficiencies, defined as the heat absorbed by the load divided by the fuel heat input, for clean ambient and clean hot WGO were found to be 30% and 31% as compared with the natural gas base-line value of 35%. Average flue temperatures were measured to be 1541 K (2314°F) for ambient WGO, 1564 K (2356°F) for hot WGO, and 1436 K (2126°F) for natural gas. The fraction of heat transferred to the load as a function of axial distance down the furnace for ambient and hot WGO relative to natural gas are shown in Figures 25 and 26. Ambient WGO and natural gas exhibit similar heat-transfer curves, while the hot WGO curve is shifted toward the flue.

For clean ambient and clean hot WGA on the baffle burner, furnace thermal efficiencies were 24% and 29% with corresponding average flue temperatures of 1453 K (2156°F) and 1503 K (2246°F). The heat-transfer curves, presented in Figures 27 and 28, manifest a shift downstream relative to natural gas for both fuel temperatures. These shifts are due to the longer flame lengths obtained with the low-Btu fuels on the baffle burner.

With the kiln burner fired at 1.03 MW_t (3.5 X 10^6 Btu/hr) the base-line natural gas efficiency was 31% with an average flue temperature of 1532 K (2298°F). Clean ambient and clean hot WGO yielded efficiencies of 29% and 30% with average flue temperatures of 1524 K (2284°F) and 1545 K (2322°F). As shown in Figures 29 and 30, the heat transfer curves for ambient and hot WGO differ somewhat from the natural gas base line and from each other. The heat-

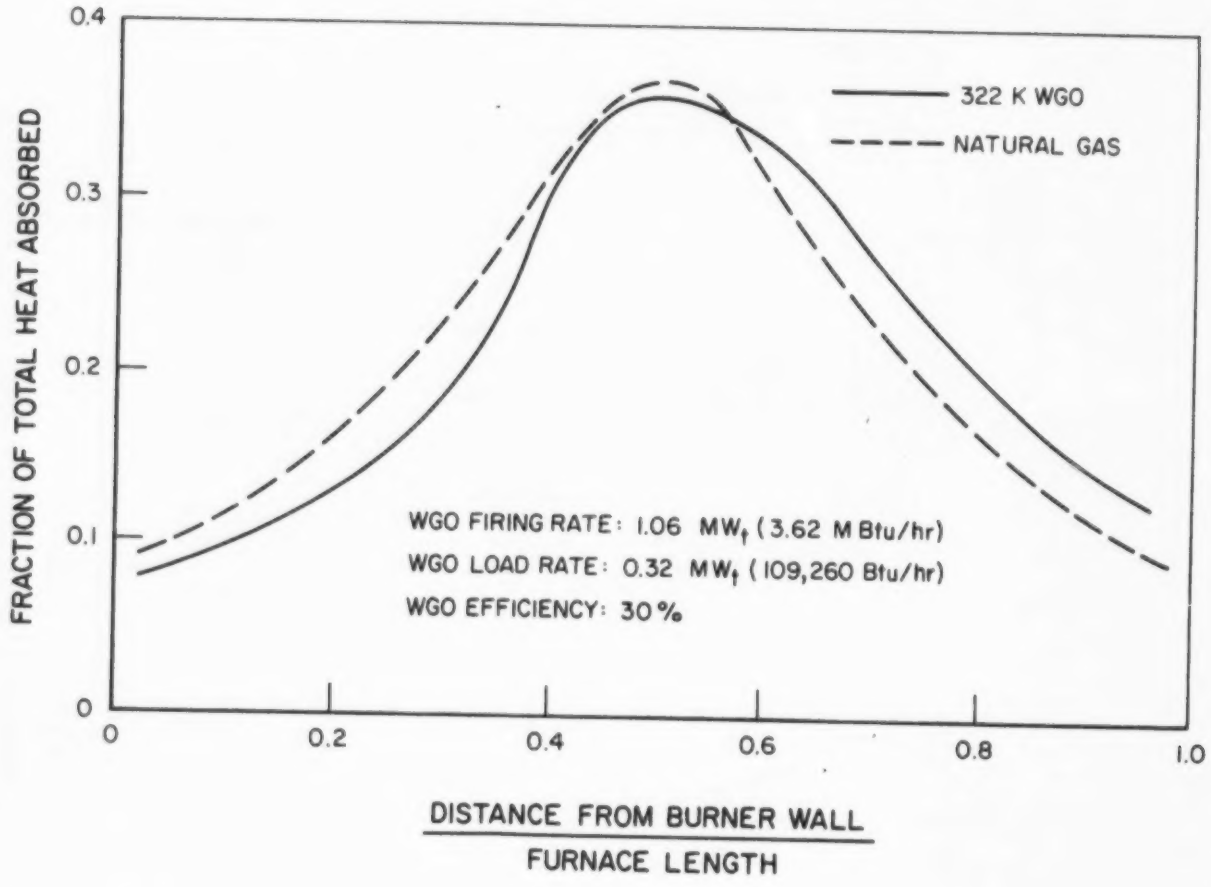

Figure 25. Heat absorption profiles for ambient, "clean" Wellman-Galusha oxygen and natural gas on the baffle burner

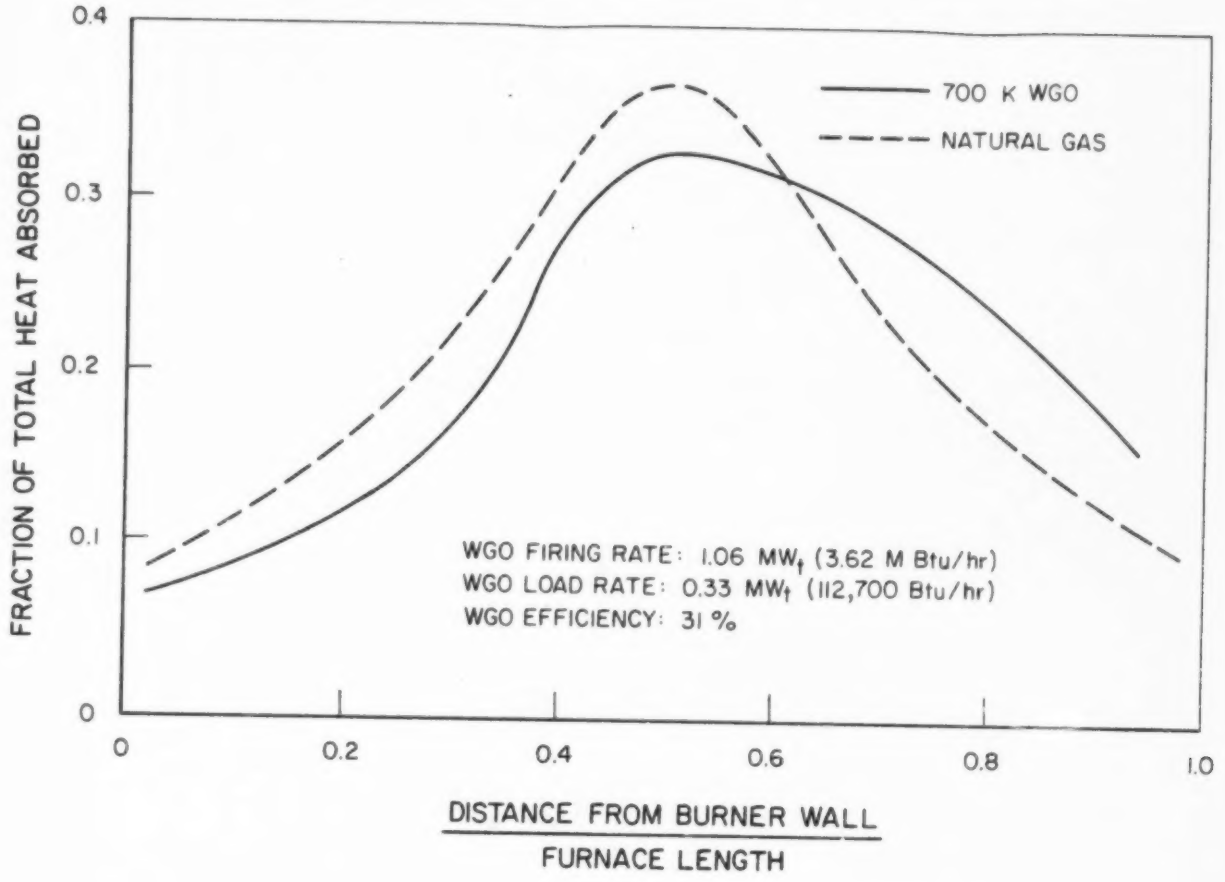

Figure 26. Heat absorption profiles for hot, "clean" Wellman-Galusha oxygen and natural gas on the baffle burner

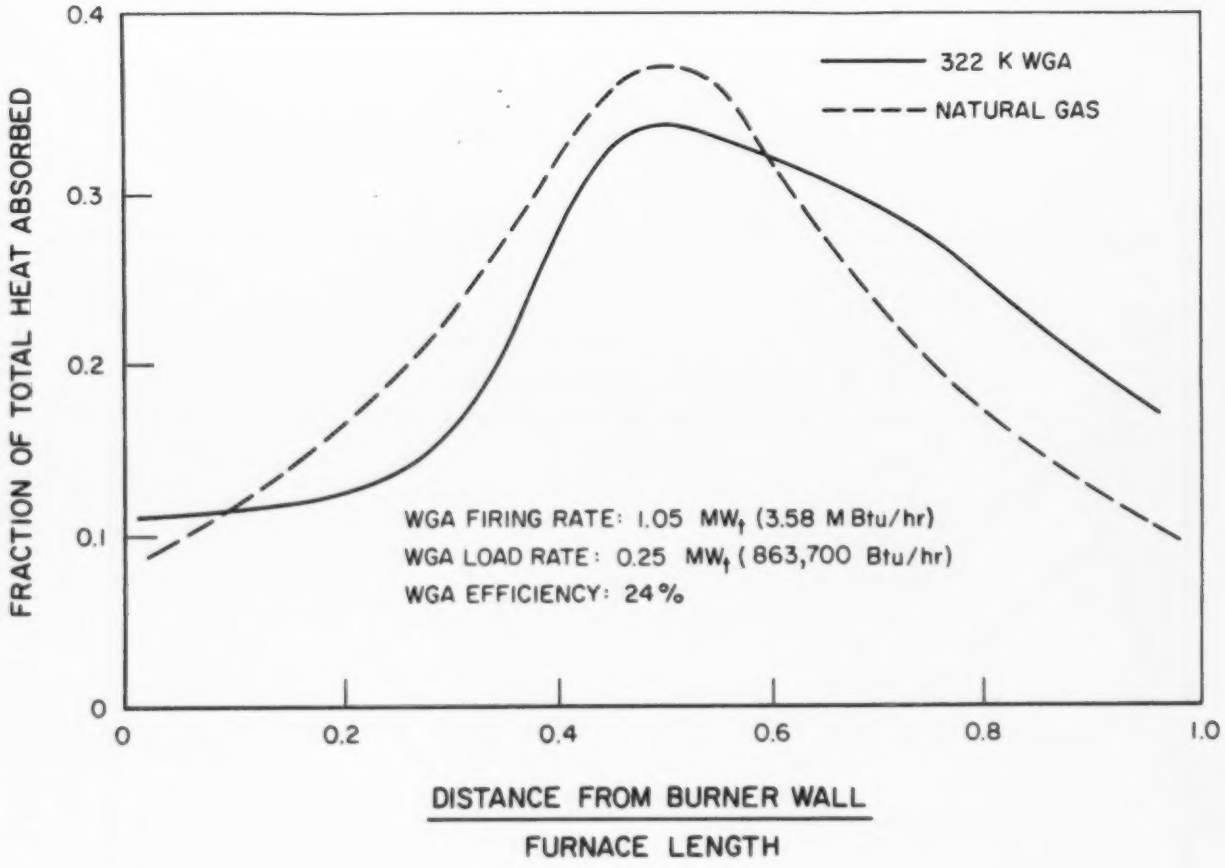

Figure 27. Heat absorption profiles for ambient, clean Wellman-Galusha air and natural gas on the baffle burner

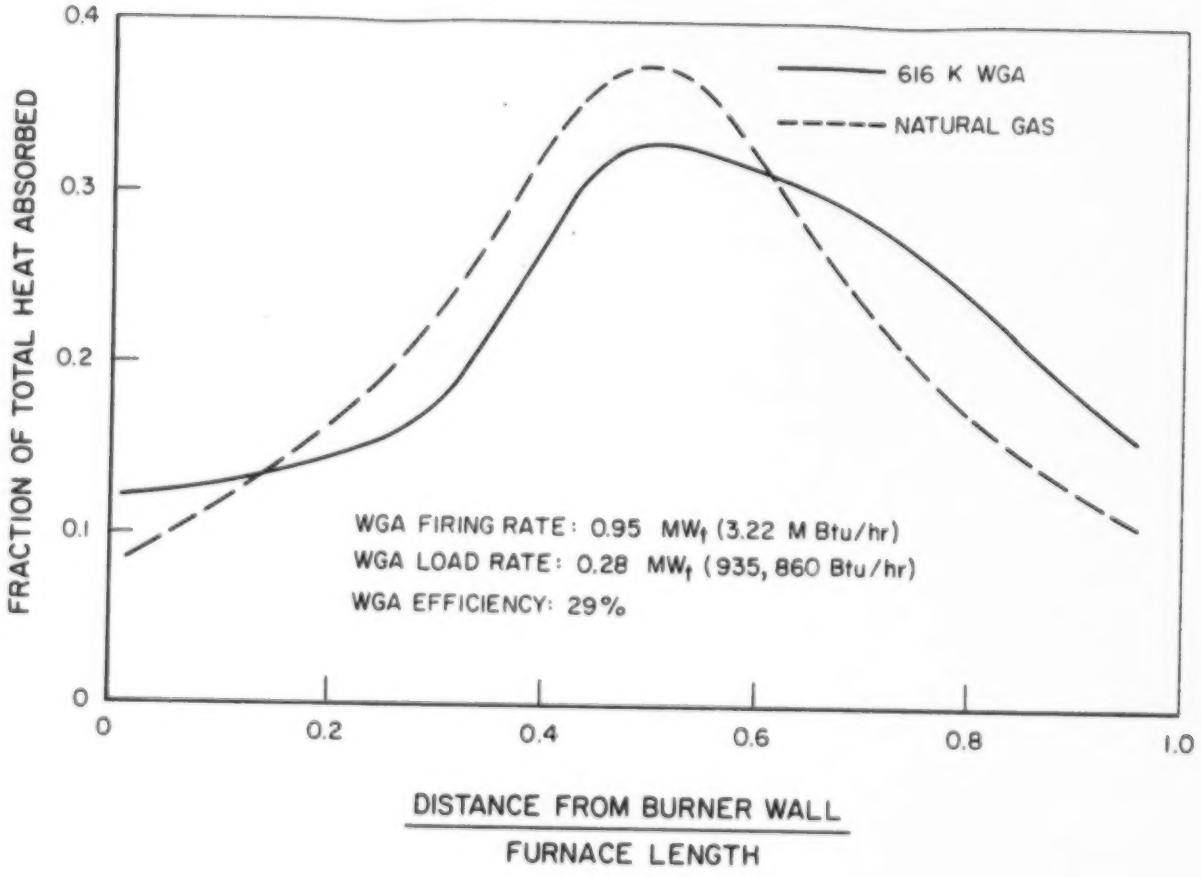

Figure 28. Heat absorption profiles for hot, clean Wellman-Galusha air and natural gas on the baffle burner

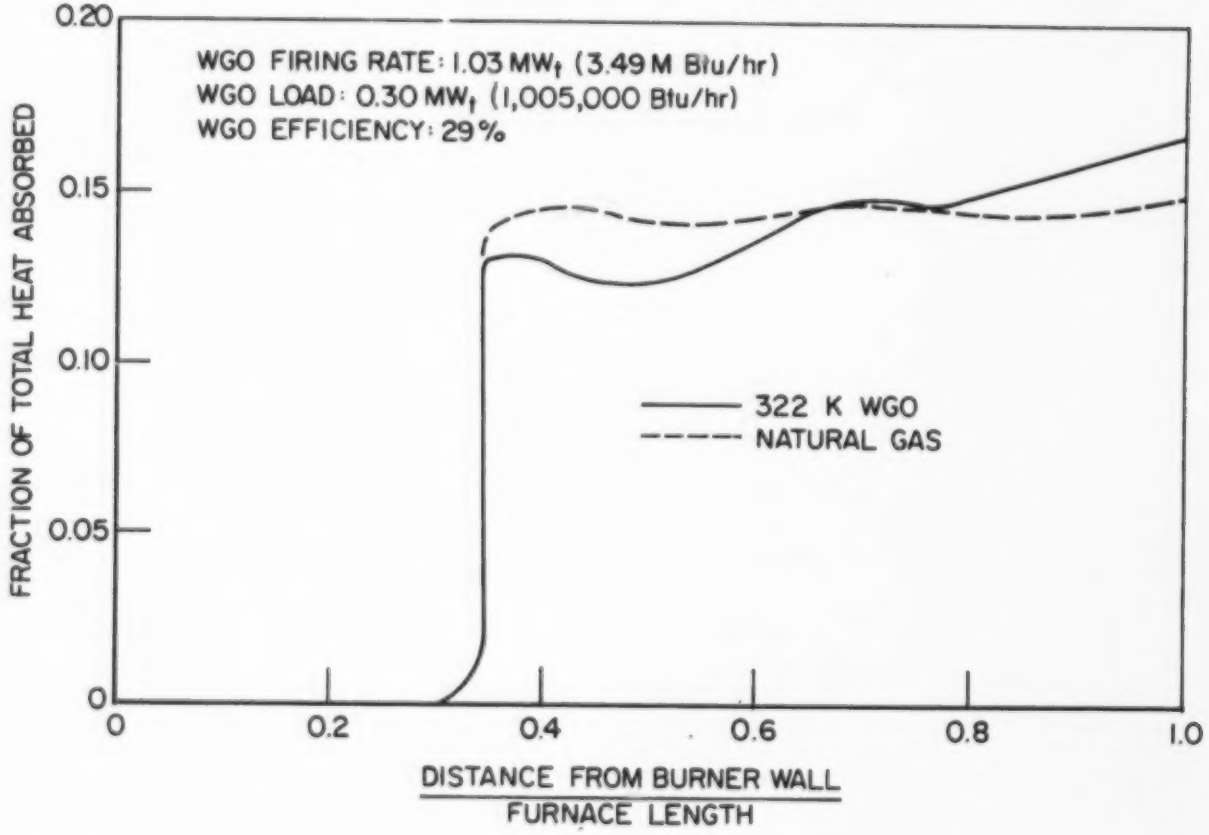

Figure 29. Heat absorption profile for ambient, clean Wellman-Galusha oxygen and natural gas on the kiln burner

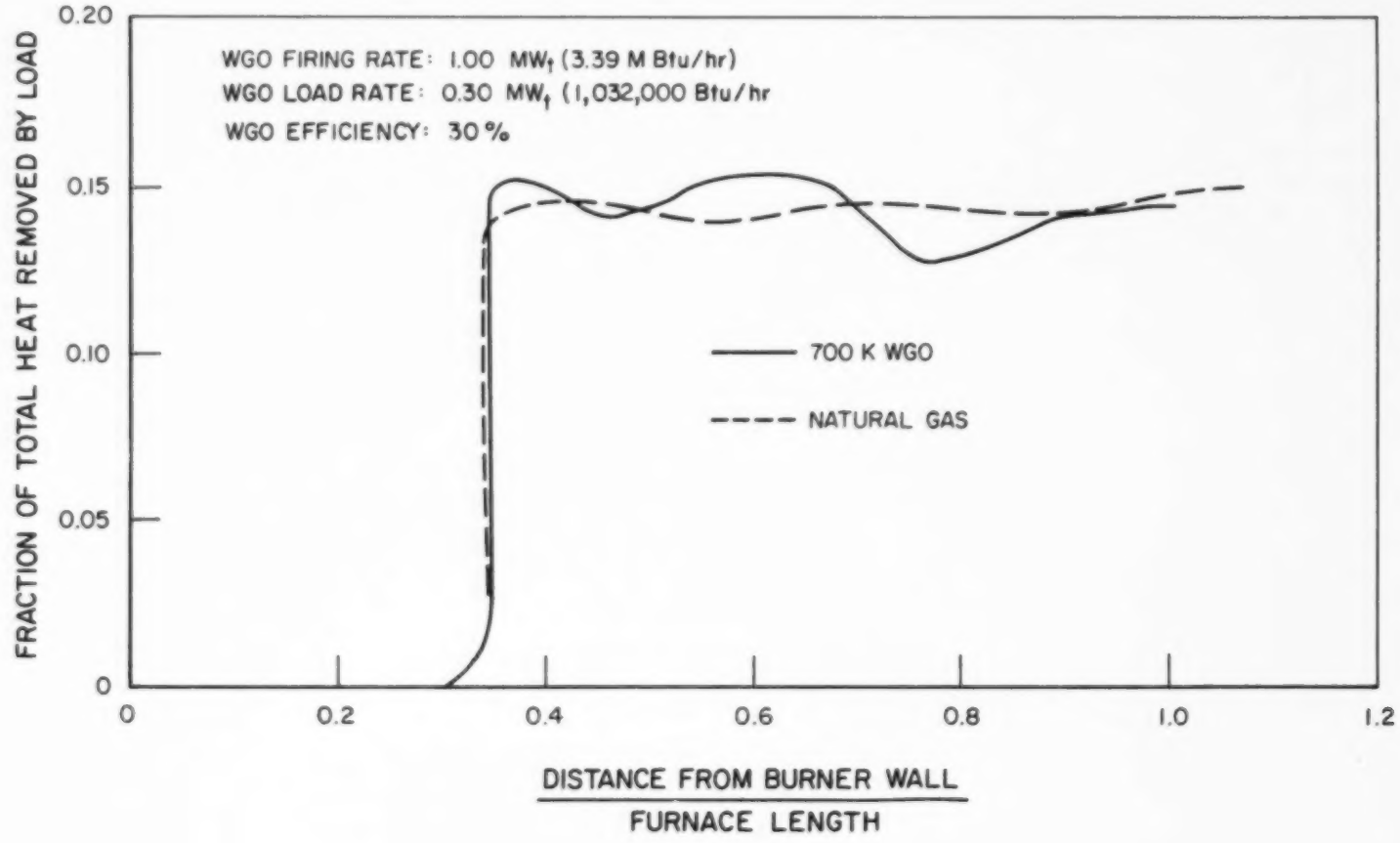

Figure 30. Heat absorption profile for hot, clean Wellman-Galusha oxygen and natural gas on the kiln burner

transfer curves for ambient WGO essentially rises continuously toward the flue, while for hot WGO the general trend of the curve approximates natural gas.

On the kiln burner, clean ambient and clean hot WGA gave furnace thermal efficiencies of 24% and 28% with average flue-gas temperatures of 1479 K (2203°F) and 1553 K (2336°F). The heat-transfer curves for ambient and hot WGA, shown in Figures 31 and 32, are comparable to that of natural gas. This similarity in heat-transfer curves is not unexpected because on the kiln burner all flame lengths were adjusted to approximate that of natural gas.

In simulating the hot raw gasifier off-gas, the addition of dopants to the clean fuel might be expected to affect overall furnace thermal efficiency in two ways. First, the ammonia, char, and tar are fuels themselves and will therefore affect the fuel heat input. Second, char and tar could affect flame emissivity.

In the studies conducted, the level of contaminant doping was such that the maximum contribution to the total fuel heat input was less than 6%. Flue temperature measurements were essentially constant for a given fuel/burner with and without doping, indicating that the doping levels employed did not significantly affect fuel heat input. In any case, calculations of furnace efficiencies included the contributions of doped material to the total fuel enthalpy.

For ammonia additions of 1.0 volume percent, no effects on furnace thermal efficiency were observed for WGO or WGA on either burner. Char addition of 0.13 g/s (0.4 grains/SCF of WGO, 0.3 grains/SCF of WGA) also had no effect on efficiency for both fuels on the burners studied.

At a tar feed rate of 0.58 g/s (1.8 grains/SCF of WGO, 1.4 grains/SCF of WGA), furnace thermal efficiencies for WGO and WGA were increased by about 1.0% to 2.0% on both burners. This enhancement is probably due to the increase in flame luminosity that was visually observed. The heat-transfer curve obtained is basically the same as for the undoped fuels.

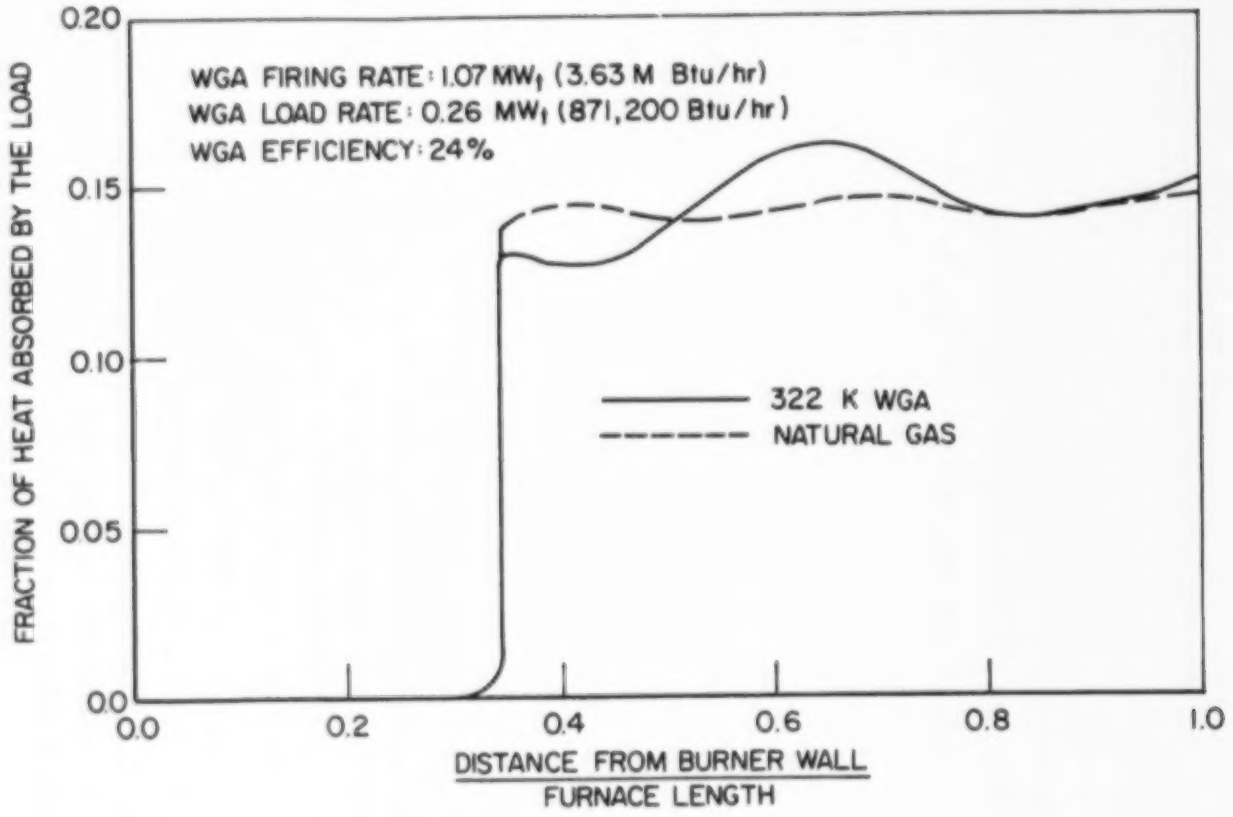

Figure 31. Heat absorption profile for Wellman-Galusha air fuel gas compared to natural gas on the kiln burner

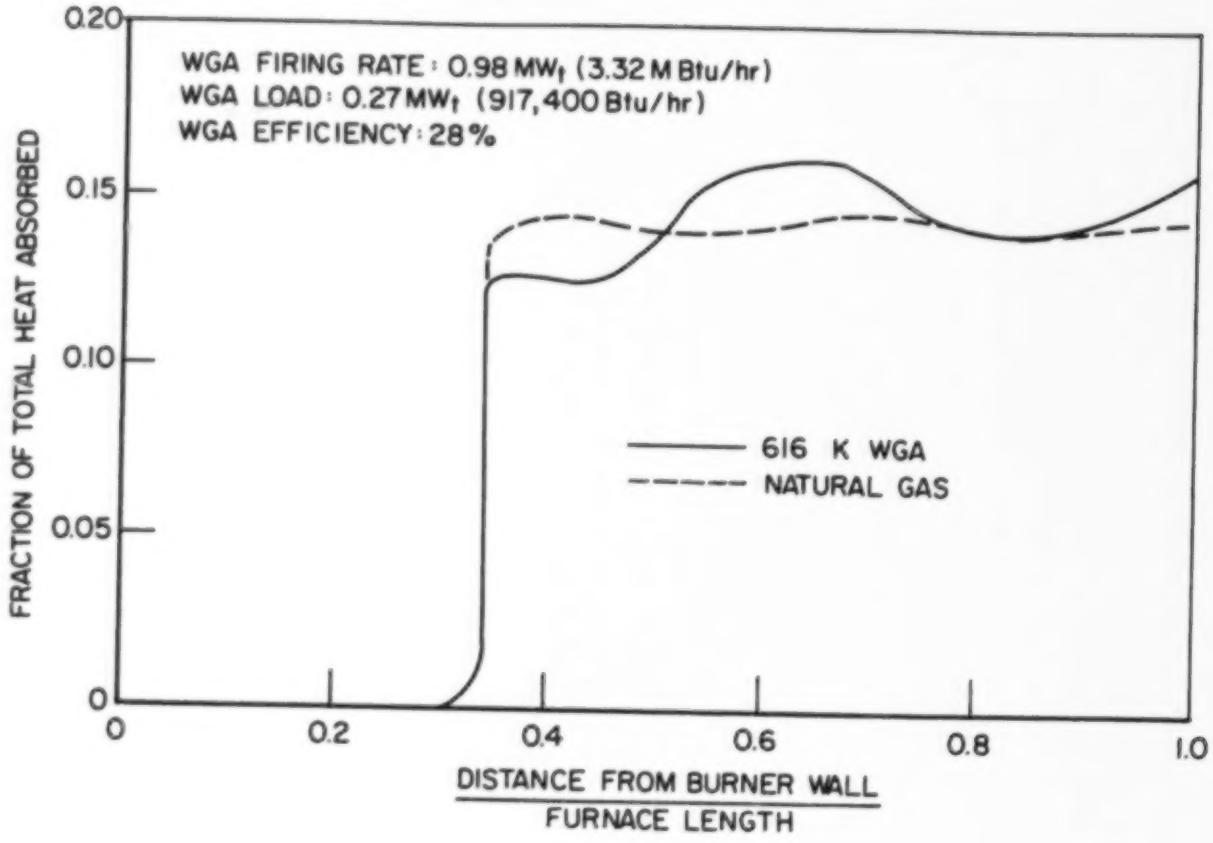

Figure 32. Heat absorption profile for hot, clean Wellman-Galusha air and natural gas on the kiln burner

DISCUSSION

FUEL-NITROGEN EFFECTS ON NO_x

In premixed flames, NO_x levels associated with thermal fixation of atmospheric nitrogen are dependent primarily on flame temperature and, secondarily, on the amount of combustion air.[4] In turbulent diffusion flames, thermal NO_x has also been found to vary with the initial degree of fuel/air mixing.[1] For the fuels and burners studied, base-line thermal NO_x levels, presented in Tables 7 and 14, are mainly ordered by adiabatic flame temperatures. Mixing effects on thermal NO_x associated with the different aerodynamic characteristics of the two burner types appear to be similar except for natural gas where a higher thermal NO_x level is found with the baffle burner than with the kiln burner, suggesting (after Reference 1) that natural gas/air mixing is somewhat better on the baffle burner.

Another source of NO_x in combustion is chemically bound nitrogen in the fuel. Since fuel-nitrogen bonds are much weaker than the bond in molecular nitrogen, fuel-nitrogen can give rise to higher amounts of NO_x than from thermal fixation.[1,4] In a flame environment, fuel-nitrogen is generally believed to react through the competitive paths[4,14]:

$$NH_i + Ox = NO \qquad (1)$$

$$NH_i + NO = N_2 \qquad (2)$$

where NH_i is some fuel-nitrogen intermediate, usually considered to be atomic nitrogen[6] or a cyano or amine derivative,[17] and Ox is an oxygen-containing species such as O, OH, or O_2. In fuel-lean combustion, fuel-nitrogen appears in the exhaust gases mostly as NO and N_2; under fuel-rich conditions, significant HCN and NH_3 can also be found.[17]

Factors that affect fuel-nitrogen conversion to NO_x are availability of oxygen, initial fuel-nitrogen concentration, temperature, and general fuel type.[4,17] As the amount of oxygen available for combustion increases, the conversion of fuel-nitrogen to NO_x increases.[18,4] Where fuel/air mixing is incomplete, this conversion is strongly affected by local oxygen concentrations as well as local flame temperatures.[13] Combustion of fuel-nitrogen under

locally fuel-rich conditions can lower the amount of NO_x formed[13] with the fuel-nitrogen preferentially forming N_2.[4] As initial fuel/air mixing is improved, the conversion efficiency of fuel-nitrogen to NO_x is enhanced.[1] For example, one group[10] reported a doubling in fuel-NO_x when going from diffusional to premixed combustion.

With increasing levels of fuel-nitrogen, the fraction converted to NO_x decreases[10,12] even though the absolute amount increases. Unlike thermal NO_x, temperature does not greatly affect fuel NO_x in premixed flames,[4] probably because overall fuel-nitrogen reactions are exothermic[1] and are therefore less temperature dependent.

Recent results[17] imply that fuel-nitrogen conversion to NO_x depends on fuel type; i.e., ammonia conversion to NO_x in hydrocarbon combustion was found to be much greater than with a hydrogen/carbon monoxide fuel. The authors attributed this to a difference in the intermediate fuel-nitrogen species (NH_i in Equation 1), depending on whether the main fuel was a hydrocarbon or not.[17]

In order to gauge the magnitude of several of the above parameters on fuel-nitrogen conversion to NO_x for raw gasifier effluents, char, tar, and ammonia were added to hot clean Wellman-Galusha fuel gases. To ascertain the contribution of each dopant to total NO_x emissions, single dopant and combination tests were also performed. The tests were performed using two industrial burners: a forward flow and a kiln burner.

With char-doped hot WGO on both burners, we have seen (Table 8) that total NO_x levels were not greatly increased above thermal at the char feed rates employed (maximum increase 30 ppm). The contribution of char-nitrogen (0.66 weight percent) to these increments is difficult to interpret, owing to the small change (if any) over thermal NO_x relative to measurement reproducibility ($\pm$ 5 ppm), and considering the known, but in this case unmeasurable, enhancement of thermal NO_x by fuel-sulfur (1.64 weight percent of char) in turbulent diffusion flames.[18] Measured SO_2 at the flue entrance accounted for about 50% of the char-sulfur in all cases. Attempts to close this sulfur balance were unsuccessful.

As with char, hot WGO tar doping results, shown in Table 9, cannot be unambiguously analyzed because of the presence of sulfur in the tar (0.47 weight percent). For the tar feed rates employed, measured NO_x exceeded the clean thermal values by about 30 ppm on both burners. This increase in NO_x cannot be solely accounted for by tar-nitrogen (0.55 weight percent) even assuming a 100% conversion to NO_x. The implication is that tar-sulfur is enhancing thermal NO_x. The contributions to total NO_x of sulfur-enhanced thermal and fuel NO_x cannot be apportioned. If all tar-nitrogen were converted to NO_x, then sulfur enhancement of thermal NO_x could be up to 10 ppm over the clean, undoped value. Conversely, enhanced thermal NO_x could be much higher, with fuel NO_x contributing relatively little to the observed increase. Measured SO_2 accounted for only 20% of tar-sulfur in all cases, while the tar residue trapped in the fuel nozzles accounted for another 10% of the fuel-sulfur.

When fuel sulfur is absent, as in the case of ammonia doped hot WGO, the effects of fuel-nitrogen on NO_x are more clearly evident. Varying the amount of ammonia in the fuel shows that the fraction of fuel-nitrogen converted to NO_x decreases with increasing fuel-nitrogen content, as can be seen from Figures 20 and 21, even though absolute NO_x levels increased. This observation is in agreement with the references cited at the beginning of this section. For example, on the baffle burner at 10% excess air, ammonia doped at 1.0 volume percent of fuel input yielded a 7% conversion to NO_x, while 0.4% ammonia gave a 14% conversion. With the kiln burner, the corresponding conversions were 8% and 16%.

Examination of Figures 20 and 21 shows that an increase in excess air, from 10% to 20%, enhanced fuel-nitrogen conversion to NO_x as expected. On the baffle burner with 1.0% ammonia in hot WGO, the conversion efficiency to NO_x increased from 7% to 8% with the increase in excess air. At the 0.4% ammonia level, the conversion went from 14% to 16%. Similar results were obtained with the kiln burner. For 1.0% and 0.4% ammonia, the respective increases in conversion with increased excess air were 8% to 10% and 16% to 17%.

At the radial flow chosen to give the proper flame length for the kiln burner (22% of the total hot WGO flow), fuel NO_x is only slightly higher than

for the baffle burner at comparable ammonia doping rates and excess air. In other words, the anticipated mixing/aerodynamic effects of the different burner types were not evident at the operating conditions employed. However, changing the amount of radial flow drastically affected ammonia conversion to NO_x, as can be seen from Figure 23. Increasing radial flow from 22% to 36% resulted in about a 50% increase in ammonia conversion, indicating that improved fuel/air mixing raises fuel-nitrogen conversion, as expected from the brief literature survey presented earlier.[1] (This effect was also confirmed when fuel-nitrogen conversion was found to be 50% higher on a highly mixed high-forward-momentum burner than on the kiln and baffle burners in other tests done at IGT.) Raising the radial flow from 0 to 15% lowered fuel NO_x. In this region, the apparent loss and then recovery of fuel/air mixedness is probably due to a trade-off between increasing radial mixing and decreasing axial fuel momentum, the net effect of which is to decrease overall mixing up to about 10% radial, where radial flow becomes the dominant mixing parameter due to the radial flow penetration of the axial flow.

Since the ammonia-to-NO_x conversion is nearly the same for the baffle burner and the kiln burner (22% radial) with the same doping rate, it may be inferred that the baffle burner gave about the same degree of initial hot WGO/air mixing as the kiln burner at 22% radial flow.

FUEL-SULFUR EFFECTS ON NO_x

As noted in the discussion of the char and tar results, fuel-sulfur is known to affect thermal NO_x. In turbulent diffusion flames, characterized by relatively poor initial fuel/air mixing, fuel-sulfur enhances thermal NO_x while in premixed flames an inhibition occurs.[18] Besides thermal NO_x fuel-sulfur also affects fuel NO_x. In premixed flames it may enhance, inhibit, or have no effect on fuel NO_x depending on the point of sampling and/or the burning mixture's residence time in the combustion apparatus, while in turbulent diffusion flames fuel-sulfur has been found to enhance fuel NO_x.[18]

In order to determine the effects of various levels of fuel-sulfur (hydrogen sulfide) on fuel-nitrogen conversion to NO_x, hot WGO, doped with 1.0 volume percent ammonia, was fired on both burners with the results shown in Figure 22. Neglecting fuel-sulfur/thermal NO_x interactions, the anticipated enhancement of fuel-nitrogen conversion during turbulent diffusion

combustion is evident at hydrogen sulfide levels of 0.5 to 2.9 volume percent fuel input. Fuel-sulfur effects on fuel NO_x are essentially the same for both burners. This is not surprising, since the kiln burner, operated at 22% radial flow, appears to give the same degree of initial hot WGO/air mixing as the baffle burner. This was also implied by the ammonia doping tests as previously noted. Further, as fuel-sulfur levels are increased the enhancement of NO_x appears to reach a maximum, as suggested by Figure 22.

On both burners, measured SO_2 corresponds to about 80% of the sulfur input (as hydrogen sulfide) at all doping rates. The fate of the remaining sulfur is uncertain. If it were present as some other species, a possible candidate is SO_3. Although equilibrium considerations predict negligible amounts of SO_3[16] in hot ($T \geq 1300$ K) combustion gases, relatively high concentrations of SO_3 are possible under combustion conditions, where rapid cooling of combustion gases can "freeze" SO_3[16,2] at superequilibrium values. Even so, reported SO_3 levels are usually only a few percent,[3] though levels as high as 10% have been recorded.[7] Such high levels are possible where quenching of SO_3 takes place by rapid cooling or by short residence time in the combustion chamber.

With hot WGO fired on the baffle and kiln burners, combustion takes place by turbulent diffusion, resulting in wide variations in local species concentrations and temperatures. The SO_2, readily formed from the added H_2S,[19] might form SO_3 in two ways: 1) by reaction with O atoms in high temperature, fuel-lean regions; and 2) in lower temperature regions ($T \geq 1000$ K) where the right-hand-side of the equilibrium process, $SO_2 + 1/2\ O_2 = SO_3$, is not negligibly small.[16] Although the SO_3/SO_2 approach to equilibrium is slow at lower temperatures[3], the presence of NO_x can catalyze the formation of SO_3 by[3,9] –

$$NO + 1/2\ O_2 \rightarrow NO_2 \qquad (3)$$

$$NO_2 + SO_2 \rightarrow SO_3 + NO \qquad (4)$$

For the tests performed with ammonia and hydrogen sulfide-doped hot WGO, high concentrations of NO_x were present, making more plausible the possibility of high SO_3. That SO_2 levels measured were not severely depressed by some artifact of the sampling system/instrumentation is supported by subsequent IGT

tests performed on a high-forward-momentum burner where measured SO_2 accounted for 95% of the hydrogen sulfide added to a 1.0 volume percent ammonia-doped low-Btu fuel (ambient WGO plus 25% N_2). Since the mixing characteristics of this kind of burner are superior to the baffle or kiln (22% radial) burners, one would expect less low-temperature formation of SO_3 if Reaction 4 is of any importance. The results are in good qualitative agreement with this tentative mechanism, though more research on this possibility is required before any definite conclusions can be made.

REFERENCES

1. Appleton, J. P. and Heywood, J. B. Fourteenth Symposium (International) on Combustion, The Combustion Institute, 1973. pp. 777.

2. Chigier, N. A. Prog. Energy Combust. Sci: 1, 3, 1975.

3. Cullis, C. F. and Mulcahy, M. F. R. Combustion and Flame, 18: 225, 1972.

4. DeSoete, G. G. La Rivista dei Combustibli, 29: 35, 1975.

5. Feldkirchner, H. L. and Schora, F. C., Jr. Coal Desulfurization Aspects of the HYGAS™ Process. Paper presented at the Second International Conference on Fluidized Bed Combustion, Hueston Woods State Park, Ohio, Oct. 4-7, 1970.

6. Haynes, B. S. Combustion and Flame, 28: 81, 1977.

7. Hedley, A. B. J. Institute of Fuel, 40: 142, 1967.

8. IGT Process Research Division. HYGAS®: 1964 to 1972, Pipeline Gas From Coal Hydrogenation (IGT Hydrogasification Process). Final Report, FE-381-T9-P3, Washington, D.C., July 1975.

9. Levy, A., Merryman, E. L., and Reid, W. T. ES&T, 4: 653, 1970.

10. Lisauskas, R. A. and Johnson, S. A. NO_x Formation During Gas Combustion. CEP, Aug. 1976. p. 76.

11. Matthews, R. D., Sawyer, R. F., and Schefer, R. W. ES&T, 11 (12): 1092, 1977.

12. Merryman, E. L. and Levy, A. Fifteenth Symposium (International) on Combustion, The Combustion Institute, 1975. pp. 1073.

13. Sarofim, A. G., Pohl, J. H., and Taylor, B. R. Mechanisms and Kinetics of NO_x Formation: Recent Developments. 69th Annual Meeting, AIChE, Nov. 30, 1976.

14. Seery, D. J. and Zabielski, M. F. Combustion and Flame, 28: 93, 1977.

15. Shoffstall, D. R. and Waibel, R. T. Burner Design Criteria for NO_x Control From Low-Btu Gas Combustion. EPA Final Report, EPA-600-7-77-094b, Dec. 1977.

16. Sternling, C. V. and Wendt, J. O. L. Kinetic Mechanisms Governing the Fate of Chemically Bound Sulfur and Nitrogen in Combustion. EPA Final Report, PB-230895, Aug, 1972.

17. Takagi, T., Ogasawara, M., Daizo, M., and Tatsumi, T. Sixteenth Symposium (International) on Combustion, The Combustion Institute, 1977. pp. 181.

18. Wendt, J. O. L., Corley, T. L., and Morcomb, J. T. Interaction Between Sulfur Oxides and Nitrogen Oxides in Combustion Processes. Second Symposium on Stationary Sources Combustion, New Orleans, Aug. 29 - Sept. 1, 1977.

19. Wendt, J. O. L. and Edmann, J. M. Effect of Sulfur Dioxide and Fuel Sulfur on Nitrogen Oxide Emissions. EPA Progress Report, Grant R-802204, Sept. 1974.

CONVERSION TABLE

ENGLISH TO SI METRIC CONVERSION FACTORS

To Convert From	To	Multiply By
10^6 Btu/hr	MW_t	2.928751 E − 01
Btu	J	1.055 E E + 03
SCFH	m^3/s	7.865790 E − 06
ft/s	m/s	3.048000 E − 01
Inch	m	2.540000 E − 02
Feet	m	3.048000 E − 01
$Feet^2$	m^2	9.290304 E − 02
$Inch^2$	m^2	6.451600 E − 04
°F	K	t°C = (t°F − 32)/1.8

J = Joule
g = gram
s = second
MW_t = megawatts thermal
m = metre
M = mega (10^6)
F = Fahrenheit
K = Kelvin
SCFH = standard cubic feet per hour